2017

Transcriptome-Wide Analysis Of Hypoxic Cancer Cells Identify Alternative Splicing As A Mechanism To Inhibit Translation

Lauren Kathleen Brady
University of Pennsylvania, labrady@mail.med.upenn.edu

Transcriptome-Wide Analysis Of Hypoxic Cancer Cells Identify Alternative Splicing As A Mechanism To Inhibit Translation

Abstract
Cellular adaptation to hypoxia involves downregulation of energy-consuming processes such as macromolecular synthesis, and leads to tumor aggressiveness and resistance to therapies for many solid cancers. To delineate mechanisms underlying this process, I carried out a transcriptome-wide study to measure hypoxia-mediated changes in gene expression and alternative splicing in in vivo and in vitro models of hypoxic head and neck carcinoma (HNC) cells. These data represent the first nucleotide-resolution study of the hypoxic transcriptome of HNC cells in vivo and in vitro. This investigation uncovered a global downregulation of genes known to regulate RNA processing, including a significant number of genes involved in splicing catalysis. Exon-level analyses classified >1,000 mRNAs to be affected by alternative splicing, and led to the discovery of a unique retained intron in the master regulator of translation initiation, EIF2B5. In this dissertation, I will describe a previously uncharacterized mechanism by which a hypoxia-mediated retained intron in EIF2B5 leads to a truncated isoform that opposes full-length eIF2Bε to inhibit translation. A functional investigation of this hypoxia-induced isoform confirmed that expression of the truncated 65kDa isoform of eIF2Bε confers a survival advantage to HNC cells under conditions of hypoxia. Moreover, expression of this isoform was observed in solid tumors of patients with HNC in a stage-dependent manner. Additional work to uncover -cis and -trans regulators of EIF2B5 splicing identified several factors that influence intron retention in EIF2B5: a weak splice site with an alternate splice site at the retained intron, hypoxia-induced expression of the splicing factor SRSF3, and increased binding of total and phospho-Ser2 RNA polymerase II (RNAPII) specifically at the intron retained under hypoxia. Altogether, these data reveal differential splicing as a previously uncharacterized mode of translational control under hypoxia and are supported by a model in which hypoxia-induced changes to co-transcriptional processing lead to selective retention of an intron containing a premature-termination codon in EIF2B5.

Degree Type
Dissertation

Degree Name
Doctor of Philosophy (PhD)

Graduate Group
Cell & Molecular Biology

First Advisor
Constantinos Koumenis

Keywords
Alternative splicing, Hypoxia, Regulation of gene expression, Translational control, Tumor microenvironment

Subject Categories
Bioinformatics | Genetics | Molecular Biology

TRANSCRIPTOME-WIDE STUDIES OF HYPOXIC CANCER CELLS IDENTIFY ALTERNATIVE SPLICING AS A MECHANISM TO INHIBIT TRANSLATION

Lauren Kathleen Brady

A DISSERTATION

in

Cell and Molecular Biology

Presented to the Faculties of the University of Pennsylvania

in

Partial Fulfillment of the Requirements for the

Degree of Doctor of Philosophy

2017

Supervisor of Dissertation	Graduate Group Chairperson
Constantinos Koumenis, Ph.D.	Daniel S. Kessler, Ph.D.
Professor	Associate Professor of Cell and
Vice Chair & Research Division Director	Developmental Biology
Department of Radiation Oncology	

Dissertation Committee

Craig H. Bassing, Ph.D.	Associate Professor of Pathology & Laboratory Medicine
Marisa S. Bartolomei, Ph.D.	Professor of Cell and Developmental Biology
	Co-Director of Penn Epigenetics Institute
Serge Y. Fuchs, Ph.D.	Professor of Cell Biology
	Director of Mari Lowe Center for Comparative Oncology
Andy J. Minn, MD, Ph.D.	Assistant Professor of Radiation Oncology

ACKNOWLEDGMENT

Foremost, I would like to extend my greatest thanks to Dr. Costas Koumenis. His willingness to openly accept me into his lab after my third year in the PhD program and continued support throughout the years was a major reason for my accomplishments in graduate school. I am especially grateful for his support to attend and present at several international research conferences, where he introduced me to leading scientists in the field of tumor microenvironment and gave me the opportunity to share our research while developing new collaborative relationships in the hypoxia community. Finally, I want to thank him for taking a risk and allowing me to pursue a project that was outside of the areas of investigation in the Koumenis Lab. He pushed and encouraged me to learn new things and to develop an interdisciplinary project which enabled us to create a high-impact manuscript. He challenged me to become a better scientist and I will always appreciate him most for that.

I extend my sincere gratitude to the members of my committee: Drs. Craig Bassing, Marisa Bartolomei, Serge Fuchs and Andy Minn. Thank you for your continued support and advice, and enabling me to develop into an independent scientist. Your positive support was a big reason why I chose to remain at Penn. I would especially like to thank Dr. Bassing for chairing my thesis committee.

I would also like to acknowledge Dr. Tom Jongens. Without his support, positive outlook and advice, I doubt that I would have made it this far.

Thank you to Dr. Vivian Cheung for introducing me to the world of RNA biology and inspiring me to start on this journey toward a PhD.

To all past and present members of the Koumenis lab: thank you for sharing in my love of science and reminding me that it is sometimes a good idea to stop and have some fun. Your support and friendship have made this a nicer experience.

Finally, I would like to extend my gratitude to my close friends and family. Thank you for your continued understanding of my dedication to this process, your loving support and for reminding me that it makes all the difference to pursue a career that I love. I certainly would not have completed this process without all of you.

ABSTRACT

TRANSCRIPTOME-WIDE ANALYSIS OF HYPOXIC CANCER CELLS IDENTIFY ALTERNATIVE SPLICING AS A MECHANISM TO INHIBIT TRANSLATION

Lauren K. Brady

Dr. Constantinos Koumenis

Cellular adaptation to hypoxia involves downregulation of energy-consuming processes such as macromolecular synthesis, and leads to tumor aggressiveness and resistance to therapies for many solid cancers. To delineate mechanisms underlying this process, I carried out a transcriptome-wide study to measure hypoxia-mediated changes in gene expression and alternative splicing in *in vivo* and *in vitro* models of hypoxic head and neck carcinoma (HNC) cells. These data represent the first nucleotide-resolution study of the hypoxic transcriptome of HNC cells *in vivo* and *in vitro*. This investigation uncovered a global downregulation of genes known to regulate RNA processing, including a significant number of genes involved in splicing catalysis. Exon-level analyses classified >1,000 mRNAs to be affected by alternative splicing, and led to the discovery of a unique retained intron in the master regulator of translation initiation, *EIF2B5*. In this dissertation, I will describe a previously uncharacterized mechanism by which a hypoxia-mediated retained intron in *EIF2B5* leads to a truncated isoform that opposes full-length eIF2Bε to inhibit translation. A functional investigation of this hypoxia-induced isoform confirmed that expression of the truncated 65kDa isoform of eIF2Bε confers a survival advantage to HNC cells under conditions of hypoxia. Moreover, expression of this isoform was observed in solid tumors of patients with HNC in a stage-dependent manner. Additional work to uncover -cis and -trans regulators of

EIF2B5 splicing identified several factors that influence intron retention in *EIF2B5*: a weak splice site with an alternate splice site at the retained intron, hypoxia-induced expression of the splicing factor SRSF3, and increased binding of total and phospho-Ser2 RNA polymerase II (RNAPII) specifically at the intron retained under hypoxia. Altogether, these data reveal differential splicing as a previously uncharacterized mode of translational control under hypoxia and are supported by a model in which hypoxia-induced changes to co-transcriptional processing lead to selective retention of an intron containing a premature-termination codon in *EIF2B5*.

TABLE OF CONTENTS

LIST OF ILLUSTRATIONS

CHAPTER 1

Introduction to regulation of gene expression

in hypoxic cancer cells

A portion of this chapter includes work previously published as the book chapter, “In Vivo Interrogation of the Hypoxic Transcriptome of Solid Tumors: Optimizing Hypoxic Probe Labeling with Laser Capture Microdissection for Isolation of High-Quality RNA for Deep Sequencing Analysis” (Brady, Popov and Koumenis, *Adv Exp Med Biol*, Vol. 899, 2016).

Reprinted with permission of Springer Nature.

Introduction

Understanding how gene expression is controlled is fundamental to identifying biological pathways and regulatory mechanisms that govern cellular responses to physiologic stresses, such as hypoxia. In the context of tumor biology, differential gene expression studies have revealed that specific features of the tumor microenvironment, such as hypoxia, influence the growth and aggressiveness of tumors (4, 5). Moreover, hypoxia has been determined to negatively impact the therapeutic response of tumors in patients (6, 7). Many of these negative effects, such as aggressiveness of tumors, arise due to the ability of cancer cells to adapt to hypoxic environments. An initial step in defining the relationship between hypoxia and tumor growth, survival and resistance to therapy is to determine how cancer cells adapt to reduced availability of oxygen in tumors. Work in this area has demonstrated that cancer cells adjust to hypoxia by downregulating energy-consuming processes, such as translation (8).

In order to advance our understanding of how cellular adaptation to hypoxia is controlled, the work described in this dissertation explores the role of alternative splicing in establishing gene expression programs that impact cellular response to hypoxia. Alternative splicing and RNA processing represent understudied areas in determining how hypoxia gene expression programs are controlled. This dissertation includes a deep investigation of changes in individual transcript levels and alternatively spliced loci to provide an additional layer of information about how gene expression is fine-tuned in hypoxic cancer cells. These data revealed novel insights into adaptation to hypoxia in head and neck cancer cells. Chapter 1 contains a summary of the history and significance of hypoxia-regulated gene expression, evolution of technical approaches to

specifically investigate hypoxic cells, and overarching scientific aims of our research to elucidate the role of alternative splicing in cellular adaptation to hypoxia.

Biological consequences of tumor hypoxia

Hypoxia, a state of reduced cellular oxygen, influences cellular survival, growth and metabolism by triggering widespread changes in gene expression (9). While transient hypoxia occurs from an imbalance between oxygen supply and consumption in normal tissues and during development, hypoxia (acute or chronic) is a key feature of solid tumors that contributes to therapeutic resistance and positively correlates with tumor aggressiveness (10). Acute hypoxia, which may last only minutes to hours, refers to fluctuation in oxygen supply due to inadequate blood flow and may only affect parts of the tumor (11). Chronic hypoxia accounts for the majority of hypoxia found in tumors. This largely occurs due to limitations in oxygen diffusion, often caused by networks of irregular vessels and increased distances between vessels in tumors compared to normal tissues (12, 13). The poor vasculature and decreased blood supply to distal regions in solid tumors creates separate, oxygen-poor microenvironments within the tumor tissue.

Hypoxic tumors exhibit resistance to radiation therapy and some chemotherapies due to lack of sufficient oxygen essential for the formation of free radicals necessary to cause DNA damage (14). Low oxygen levels and associated tissue acidity also decrease cellular uptake of chemotherapies and result in reduced drug delivery to tumors (14). Moreover, development of blood vessels is tightly regulated by expression of pro-angiogenic factors (i.e. VEGF) and anti-angiogenic factors (i.e. thrombospondin), which respond to demand for oxygen and nutrients. Expression of these and other angiogenic-

related factors is regulated by the Hypoxia Inducible transcription Factor HIF-1 (15). Overexpression of pro-angiogenic factors and increased cellular growth rates often disrupts the network and structure of blood vessels in tumors. Uncovering a deeper knowledge of which genes and isoforms are differentially expressed in hypoxic regions of tumors will provide a better understanding of how pathways that impact resistance to therapy, such as angiogenesis, are regulated.

Using hypoxia gene expression signatures to understand the biology of the tumor microenvironment

There are several solid tumors that are considered more hypoxic than others, such as: gliobastoma multiforme, head and neck carcinomas, breast, cervix and prostate (16-18). Due to the biological pathways that undergo changes in gene expression under hypoxia, there is a negative correlation between the level of hypoxia in tumors and overall survival in patients of many solid cancers, including head and neck squamous cell carcinoma (HNSC) (19). Pioneering work to establish a hypoxia "metagene" signature used microarray data from patients with HNSC and discovered a subset of genes whose expression that strongly correlated with levels of tumor hypoxia (20, 21). Currently, hypoxia "metagene" expression signatures are accepted as a surrogate method to classify tumor hypoxia for HNSC and other solid malignancies, including breast and prostate cancer (20, 21).

Even though regulation of mRNA and miRNA have been extensively studied *in vitro* (22, 23), *in vivo* analysis of hypoxic tumors has been limited due to small quantities of poor-quality RNA when isolated from immunohistochemical samples using traditional

methods. Although *in vitro* hypoxic conditions can represent oxygen levels in tumors, these conditions do not take into the account many other factors present in the tumor microenvironment that contribute to physiologic stress like low nutrient levels, low pH, infiltrating immune cells and necrotic tissue, or, more critically, the interplay between these factors and the effect on gene expression. A prime example of this is lactic acidosis, which when it co-occurs with hypoxia, results in reduced stabilization of HIF-1 and counteracts the usual induction of hypoxia-responsive genes. This occurs in part due to lactic acidosis stimulating the Unfolded Protein Response (UPR) as well as an inflammatory response (24).

Studying changes in gene expression due to stresses that arise in the tumor microenvironment, such as hypoxia or acidosis, can be simplified by utilizing *in vitro* systems. The value in utilizing *in vitro* approaches is that it enables the isolation of specific stresses within the tumor microenvironment, such as hypoxia. However, it is crucial to pair these studies with the respective *in vivo* models to gain a more complete understanding of the basic biology of the tumor microenvironment. As a result, there is an immediate need for improved methods to isolate DNA and RNA from tumor samples. To achieve this goal, our group previously developed an approach utilizing a combination of EF5 staining, laser-capture microdissection (LCM) and modification to traditional RNA purification methods to specifically isolate high-quality RNA from hypoxic and normoxic regions for gene expression studies (25). Imaging techniques utilizing oxygen-sensitive molecules followed by immunofluorescence staining offer the advantage as being a safe and non-invasive method for identifying hypoxia in patient tumors. EF5 is an FDA-approved fluorinated derivative of etanidazole, that is reduced in regions of hypoxia where it covalently binds to adjacent proteins and DNA. This stable

binding makes EF5 ideal for use as ^{18}F-EF5 for PET scans in patients or animals, or allows for subsequent staining with anti-EF5 antibodies conjugated to fluorochromes, such as Cy3 or Cy5, for downstream microscopy-based applications at the bench (26). EF5 is also a lipophilic molecule that is readily taken up by tumor tissue. Moreover, its binding does not rely on pH, both features which offer the advantage of increased biodistribution compared to other hypoxia markers (26). Use of molecular hypoxia markers have enabled the collection of clinical data to strengthen the finding that hypoxic tumors are indeed correlated with poor prognosis. In addition, these methods allow safe and precise staining of hypoxic tissues, which in combination with the laser-capture microdissection (LCM) technology, has allowed for the optimization and development of downstream methods for excising high-quality RNA for gene expression analyses.

Marotta et al., were the first to publish on use of LCM to extract high-grade RNA from specific hypoxic and normoxic tumor sections for subsequent microarray analysis. Specifically, gliosarcoma cells were used to establish tumors in a rodent model. The bioreductive dye, EF5, was used to specifically label hypoxic regions of the tumor tissues, allowing for the study of gene expression differences across normoxic and hypoxic tissues from the same tumor (25). This same approach was used to carry out RNA-sequencing of normoxic and hypoxic tissues of a murine model of head and neck cancer (see Figure 1A-E for overview). I used these data to investigate hypoxia-mediated changes in regulation of alternative splicing, which is described in Chapter 2. In addition, several variations were made to the protocol to specifically enrich for mature mRNAs (Figure 1D,E). First, oligo-dT selection was used to specifically enrich for poly-adenylated mature mRNAs (which comprise only 3-5% of total RNA) for the specific goal of evaluating gene expression and mRNA splicing. Additionally, an enzyme treatment was used to deplete the samples of

ribosomal RNAs, which can account for as much as 80% of the total RNA material in the cell (27).

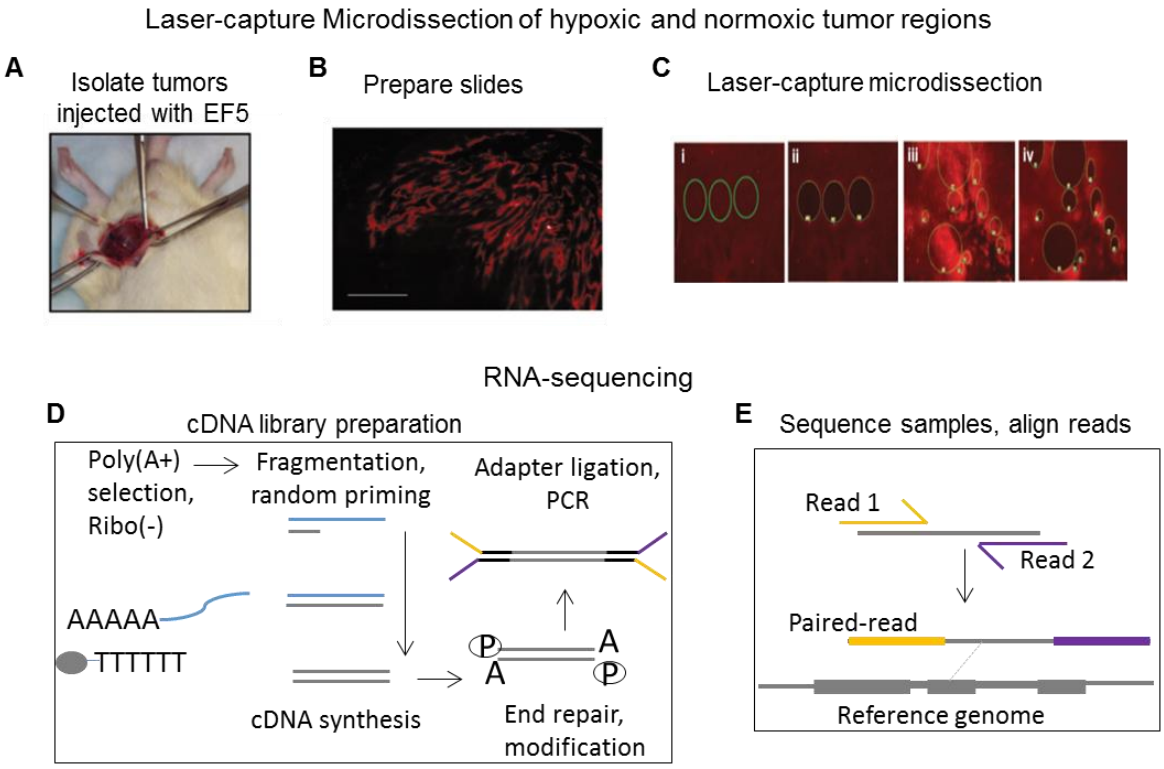

Figure 1.1: Experimental overview for *in vivo* labeling paired with LCM for RNA sequencing of hypoxic tumors. A: Representative image of injection of EF5 into an animal model of tumor hypoxia. B: After tumor is excised, membrane slides are prepared with antibodies against EF5 to visualize areas of hypoxia, stained in red. C: Laser capture microdissection (LCM) can then be used to remove normoxic ((i) pre-LCM, (ii) post-LCM) and hypoxic ((iii) pre-LCM, (iv) post-LCM) tissue. Panels a–c modified from [23]. D: Following RNA extraction, cDNA libraries are prepared using mRNA depleted of rRNAs and annealed with primers specific for the sequencing platform. E: Libraries are sequenced and the sequences are aligned to a reference genome.

Regulation of mRNA levels in hypoxic tumors

There are several mechanisms that cooperate to control mRNA levels in hypoxic cells. Understanding how the expression response to hypoxia is controlled is the basis to identifying which pathways mediate the cellular adaptation to hypoxia and identifying methods to target these pathways in tumors for therapeutic benefit. Hypoxia-responsive genes have historically been studied in relation to the major Hypoxia Inducible transcription Factors (HIFs). HIF-1, is a heterodimeric protein which includes an oxygen-responsive alpha subunit and constitutively active beta subunit. Under normoxic conditions, HIF-1 is constantly synthesized and degraded (28). In the presence of normal oxygen concentrations, HIF-1 is hydroxylated on proline residues, where it interacts with von Hippel-Lindau factor (VHL), becomes ubiquitinated and is eventually degraded via the proteasome. Hydroxylation also prevents co-factor binding to HIF-1a, further inhibiting its transcription regulatory function. Decreased oxygen prevents this process, which results in stabilized HIF-1 protein (28, 29). These conditions permit HIF-1a proteins to heterodimerize with a beta subunit and induce transcription of target genes involved in glucose metabolism, cell survival and cell migration (30).

Some well-known examples of HIF-1α transcriptional targets are vascular endothelial growth factors (VEGF) involved in angiogenesis, GLUT1, also known as SLC2A, glucose transporter involved in glycolysis, and carbonic anhydrase IX (CA9), which is a regulator of cellular pH (31). Expression of these and other HIF-1α regulated proteins also correlate with the metastatic potential of tumors and therapeutic resistance (32).

Translational control in hypoxic cells

Transcriptional activation of hypoxia-responsive genes represents one component of how mRNA levels are controlled under conditions of low oxygen. However, various regulators in addition to transcription factors, including RNA binding proteins (RBPs) and non-coding RNAs, influence the stability and localization of mRNAs under hypoxia (33-35). For example, the RBPs HuR and PTB bind to major regulators of hypoxic response such as HIF1α (36, 37) and miRNA-199a (38) to regulate stability and localization of these RNAs. Factors such as these directly impact the potential of an mRNA to be translated. Moreover, both nonsense-mediated decay (NMD) and translation are globally downregulated in hypoxic cells in an eIF2α phosphorylation-dependent manner (8, 39). In the context of hypoxia, phosphorylation of eIF2α is mediated by the kinase, PERK (8); however, other activators of the unfolded protein response (UPR) such as nutrient deprivation, also induce phosphorylation of eIF2α by GCN2 (40, 41).

The NMD pathway is an evolutionarily conserved mechanism to identify transcripts that contain premature-termination codons (PTCs) and initiate the decay of these transcripts to prevent their translation into proteins. Typically, NMD surveillance recognizes stop codons as premature if the stop occurs more than 50 nucleotides upstream of a splice junction (42). Bioinformatic analyses have approximated that up to 20-35% of alternatively spliced transcripts could contain PTCs and become targets of nonsense mediated decay (NMD) (43, 44); however in conditions where NMD is inhibited, transcripts can escape decay and become translated into truncated proteins (45).

One of the chief ways that tumor cells overcome hypoxic stress is by downregulating translation which was demonstrated to be critical for cell survival under

extreme hypoxia (8). Under conditions of normal oxygen, protein synthesis requires the five-member eIF2B complex, which binds eIF2α and exchanges GDP for GTP to initiate translation (46, 47). The eIF2Bε subunit is a necessary component of this complex which contains both the active guanine nucleotide exchange factor (GEF) domain and a region for association with eIF2α (47). In conditions of hypoxia, eIF2α is phosphorylated (8) and translation initiation is unable to occur when eIF2B complexes bind phospho-eIF2α. However, this phosphorylation can be removed by GADD34 and is not long-lasting (48, 49). Intriguingly, in cells stably expressing a form of eIF2α with an S51A mutation rendering these cells unable to be phosphorylated, translation initiation resumed under hypoxia, but only to approximately 75% of the level observed in control cells (8). These data suggested the existence of additional mechanisms to sustain reduced protein synthesis in hypoxic cancer cells. Chapter 3 will describe how an investigating of hypoxia-mediated changes in splicing uncovered a previously uncharacterized hypoxia-responsive isoform of eIF2Bε which acts to inhibit translation and promote survival of hypoxic cancer cells.

The role of alternative splicing in the cellular response to hypoxia

There is strong evidence to support that alternative splicing represents an additional layer of control in the regulation of hypoxia gene expression programs. Initial studies have identified select targets of HIF-1a to undergo alternative splicing (50). Moreover, hypoxia-induced changes in the expression of certain non-coding RNAs occur due to splicing and may impact regulation of the DNA damage response in conditions of low oxygen (51). Moreover, HIF-1α impacts the splicing of several of its transcriptional

target genes, including ADM and CA9 (50, 52). It remains unclear what the biological consequences of altered splicing in hypoxic tumors may be and what HIF-independent factors regulate splicing in the hypoxic tumor microenvironment. These two understudied areas of hypoxic biology were a major inspiration for the scientific goals of this dissertation, which I will explain in greater detail at the conclusion of Chapter 1.

Mechanistically, a connection between regulation of RNA splicing and altered signaling within the tumor microenvironment has recently emerged; several major signaling pathways known to be overactive in cancer which impact cell growth, survival and angiogenesis, also impact expression and processing of mRNA isoforms (53). Several kinases known to phosphorylate major RBPs and splicing factors are also hypoxia-responsive (54). In addition, some splicing factors, including SF3B1, are upregulated in a HIF1α-dependent manner under physiological conditions of hypoxia in cardiac myocytes (55); however, it remains unclear precisely how mRNA splicing is regulated during periods of oxygen deprivation in cancer cells and what the resulting biological implications are. While regulation of RNA splicing can be varied in a tissue-specific or under physiologic stress, it is important to begin with a summary of what has been fully characterized about this process in normal cells.

Regulation of mRNA splicing & determinants of intron retention

Splicing is the biochemical reaction by which introns are removed from pre-mRNA to result in mature messenger RNAs typically consisting of exons and terminal untranslated regions (UTRs) (56). This reaction is catalyzed by the spliceosome complex of RNA-bound proteins, RNPs, which recognize and bind conserved RNA sequences, and is

influenced by additional RNA binding proteins such as splicing factors (56). For more than 99% of mRNAs, splicing occurs via assembly of the major spliceosome containing five small nuclear ribonucleoprotein or snRNP complexes (as reviewed in (57)). Briefly, this process entails U5 and U4/U6 tri-snRNP assembly, followed by U1 binding at the 5' splice site, U2 binding at the branch-point sequence and U2AF binding at the 3' splice site (Figure 2). This step is broadly defined as exon definition and is largely influenced by highly conserved -cis RNA sequences. These sequences include the splice sites, intron sequence around the branch-point sequence and splicing enhancer or silencer sequences located in introns or exons, and often impart a stronger influence when located near a splice site (58). Generally, the enhancer and silencer motifs are bound by serine/arginine-rich (SR) proteins and heterogeneous nuclear ribonucleoproteins (hnRNPs) to promote or repress splicing, respectively (59, 60).

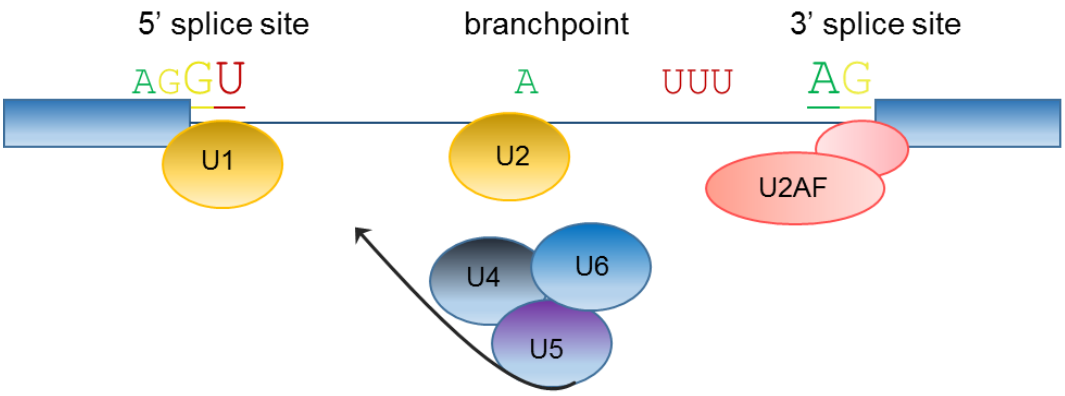

Figure 1.2: Conserved sequences involved in the regulation of RNA splicing. The conserved splice sites are highlighted at each of the exon junctions flanking this intron. Exons shown as blue rectangles and intron depicted as blue line drawn in between. Regulatory RNA/protein complexes shown and labeled below.

Although these sequences are highly conserved, variation in the splice site can also influence splicing efficiency and splice site choice. For example, weak splice sites may contribute to inefficient splicing or promote usage of alternate splice sites under specific conditions, such as changes to the elongation rate of RNA polymerase II (RNAPII) (61). The splicing of many genes is sensitive to changes in the activity of RNAPII since splicing occurs co-transcriptionally. The kinetics of elongating RNAPII influences the spliceosome interaction with RNA, such that slower or faster RNAPII can alter mRNA splicing patterns. This was best described in a genetic model of RNA polymerase elongation rate mutants, in which cells expressing a slower elongating RNAPII exhibited an increase in retained introns which contained relatively weaker splice sites as opposed to introns unaffected by a slower transcription rate (61).

In combination to the role of -cis RNA sequences in determining splice site decisions, changes in cell signaling alter the expression and activity of splicing factors. More than 95% of multi-exonic genes can be alternatively spliced in a tissue-specific context or due to changes in cellular signaling triggered by physiological or extrinsic stresses. For example, global downregulation of many key splicing factors, including SF3B1 leads to intron retention as a mechanism to promote maturation of granulocytes during hematopoiesis (3). Since many of the same biological pathways that contribute to normal development also influence tumor development, it is unsurprising that over-active signaling networks in tumors can significantly impact patterns of mRNA splicing.

Altered regulation of splicing in cancer

Many of the fundamental pathways that affect normal tissue and tumor development are influenced by over-active signaling networks. In tumors, some of these signaling networks lead to overexpression of kinases which act to phosphorylate and influence biological processes within the tumor microenvironment. A key implication of hyper-activated kinases is their impact on factors that regulate mRNA processing and splicing. For example, many tumors contain activated EGFR signaling, which leads to induction of kinases, such as SRPK1 and CLK1. These kinase activate the major class of serine-arginine rich splicing factors (including SRSF1, SRSF2 and SRSF3) which mediate splicing and expression of mRNA isoforms involved in apoptosis, cell growth and angiogenesis (reviewed in (53)).

Interestingly, SF3B1 is described as the most commonly mutated splicing factor in cancer (62). This splicing factor is critical and suggested to be involved for recognition of nearly all 3' splice sites (63). Mutations in SF3B1 have been observed in patients with leukemia, pancreatic cancer, uveal melanoma, breast cancer and bladder cancer (62). Many additional splicing factors even when unmutated may act as proto-oncogenes. Key examples include SRSF1 and SRSF3. In breast cancer, increased levels of SRSF1 lead to alternatively spliced isoforms of *BIM* and *BIN1* that become unable to carry out their pro-apoptotic functions (64). Decreased levels of SRSF3 lead to an isoform of p53 that initiates p53-induced senescence (65).

Collectively, these studies have identified common genome-wide alterations in patterns of splicing, including an increase in retained introns in tumors relative to normal tissues (66, 67). Yet how intron retention is controlled in cancer cells remains poorly

understood. Exploring the functional consequences of intron-containing transcripts and investigating regulators of intron retention in the context of hypoxic cancer cells are overarching aims of the research in Chapter 3.

Scientific Aims: Investigating the link between hypoxia & alternative splicing

The overall goal of this work is to characterize alternative splicing in hypoxic cancer cells, gain mechanistic insight into this process and identify the most biologically impactful hypoxia-responsive mRNA isoforms. Based on previous data describing various stress-responsive proteins in addition to transcription factors that influence mRNA levels in hypoxic cells, my overarching hypothesis is that hypoxia leads to widespread changes in regulation of alternative splicing in head and neck cancer cells. For the first aim of my dissertation, I set out to measure changes in alternative splicing in *in vivo* and *in vitro* models of hypoxic HNSC cells at nucleotide resolution. In the second aim of this dissertation, my goal was to carry out a functional investigation of the biological impact of select hypoxia-responsive isoforms. One of the strongest candidates that arose from the data was a hypoxia-induced retained intron in the major regulator of translation initiation, *EIF2B5*. I hypothesized that under conditions of hypoxia, retention of this intron creates a premature-termination codon resulting in a truncated protein isoform of eIF2Bε. This truncated isoform was predicted to lack the functional GEF domain, thus I tested if the hypoxia-induced truncated isoform of eIF2Bε acted opposite to the full-length isoform to inhibit translation.

Regulation of intron retention has been identified as a way to fine-tune gene expression during development (3). Widespread retention of introns has also been

observed in most solid cancers (66). The work described in Chapters 2 and 3 further establishes the role of mRNA splicing in cellular adaptation to hypoxia and identifies intron retention as a component of gene expression regulation in hypoxic cells. Chapter 2 specifically characterizes changes in individual mRNA transcript levels and begins to explore how regulation of RNA processing and mRNA splicing is altered in hypoxic cells *in vivo* and *in vitro*. Data from Chapter 3 will include a deeper exon-level analysis of alternative splicing by examining splice junction reads to study expression levels at specific loci that change under hypoxia. This analysis allowed me to address scientific questions such as, are there particular types of splicing (such as skipped exons or retained introns) that are differentially regulated in hypoxic cells? What is the biological consequence of hypoxia-mediated changes in splicing? And do any of these changes in splicing lead to protein isoforms that differ in function compared to the isoform(s) expressed in normoxic conditions?

Conclusion

The additional layers of biological information that are uncovered by deeply sequencing tumor RNA in combination with *in vitro* samples to specifically study the effects of hypoxia will bring insight into control of splicing in hypoxic cancer cells. The novel findings which will be presented in the following chapters highlight the significance of examining regulation of gene expression at nucleotide resolution to identify stress-responsive isoforms which carry out critical biological functions under specific conditions. Here, I present a functional investigation of the role of a hypoxia-induced dominant-

negative isoform of eIF2Bε as one of the first examples of how splicing can contribute to cellular adaptation to hypoxic stress.

CHAPTER 2

Transcriptome analysis of head and neck cancer cells

in vivo & *in vitro* identifies downregulation

of RNA processing & splicing under hypoxia

Introduction

Tumor hypoxia strongly correlates with reduced overall survival in patients of many types of cancer, including head and neck (68). Uncovering how hypoxia contributes to tumorigenesis and leads to poor prognosis has proven to be a multi-faceted and complicated research goal. Advances in techniques to specifically label and probe hypoxic cells for gene expression profiling have led to the identification of well over 1,000 hypoxia-responsive genes (25). A smaller subset of these genes, including key regulators of pathways impacting angiogenesis, oxygen metabolism, cell migration and protein synthesis, are universally and robustly regulated across different solid tumor types, including breast, head and neck, and prostate (20, 21). Differential expression of these genes has been used as a marker in lieu of other invasive methods to identify and quantify hypoxia in tumor samples from patients to gain prognostic and biologic data. This information has the potential to guide treatment options for patients if scientists can identify the genes underlying hypoxia-mediated resistance to therapy and metastasis, but this goal has yet to be realized due to several obstacles. Two of the greatest challenges in applying this basic research to the clinic include developing a system to investigate hypoxia within the tumor microenvironment without using whole, homogenized tumor samples (which do not account for tissue heterogeneity); and identifying precisely which genes are targetable for impacting the largest effects on tumor survival and response to treatment. Additionally, as greater than 90% of human genes can be expressed as multiple mRNA isoforms which often yield protein isoforms with distinct functions (69, 70), there is a need to expand current gene expression studies to include isoform-level changes.

To address these challenges, I utilized data obtained using a method previously developed by our group which enabled the first characterization of hypoxia-induced changes in gene expression from *in vivo* samples (25). This method uses laser capture microdissection (LCM) of tumors injected with the FDA-approved hypoxia probe EF5, which is an established and effective way to identify hypoxic areas of tumors in both patients and animal models of cancer (71). This probe readily diffuses into tumors where it is reduced to an active radical exclusively in oxygen-poor regions, and covalently binds with surrounding proteins and DNA. Using this method, RNA was isolated from normoxic and hypoxic regions of head and neck tumors established in mice for deep sequencing. To build upon this study and allow for the controlled isolation of effects due to hypoxia alone, I also prepared corresponding *in vitro* samples. Together, these data enabled me to investigate regulation of gene expression and mRNA splicing in hypoxic head and neck cancer cells at base-pair resolution.

Surprisingly, although alterations in splicing have been observed in several cancers and occur in pathways which influence (and are influenced by) tumor hypoxia, the regulation of splicing in hypoxic tumors and the impact of hypoxia-responsive isoforms on tumor survival and patient outcome has yet to be investigated genome-wide. For example, the major splicing factor SF1 is directly upregulated transcriptionally in cancers with overexpressed c-Myc transcription factor. This in turn mediates splicing of key genes such as Bcl family members and Caspases involved in cell death, *VEGF* genes involved in angiogenesis and additional genes impacting invasion and metastasis (53). Additionally, a handful of genes have been described as alternatively spliced in hypoxic cancer cells, including core target genes of the hypoxia-inducible transcription

factors (HIFs), such as the pyruvate dehydrogenase kinase, *PDK1* (50); however, the biological impacts of these changes have yet to be evaluated.

My goal is to investigate the link between hypoxia, splicing and cell survival in a model of head and neck cancer and will begin by assessing whether select alternatively spliced isoforms establish properties of the hypoxic tumor microenvironment, such as reduced protein synthesis (which is described in greater detail in Chapter 3). Head and neck cancer (HNC) is one of the solid malignancy most adversely affected by hypoxic fractions. Because patients affected by HNC have been deeply studied at a genetic level to uncover molecular markers of hypoxia (21), HNC is a model disease system in which to investigate the biology of hypoxic tumors. Initial work in this area importantly established that the level of hypoxia in tumors of HNC patients was associated with a strong and reproducible hypoxia "metagene" signature, comprised of many HIF-1α activated genes yet also including some genes consistently repressed under hypoxia. Gene expression data from a large cohort of HNC patients confirmed that patients with the strongest hypoxia metagene signatures exhibited significantly reduced overall survival compared to those with weaker metagene signals (21). Moreover, these initial studies have been expanded to verify that the hypoxia metagene initially described in HNC is quite robust and nearly universal, and was further refined to successfully classify patients affected by additional solid cancers, including breast and prostate (20).

To gain a deeper understanding of the biology of hypoxia in HNC, RNA was isolated from normoxic and hypoxic regions of tumors established in athymic mice from human head and neck squamous cell carcinoma SQ20B cells and used for deep sequencing. For this study, the bio-reductive dye, EF5, was used to specifically label oxygen-deprived areas of tumor tissue. EF5 was selected as a cellular hypoxia label

because it is an FDA-approved molecule that has been used in the clinic to safely label hypoxic tissues in patients (26). RNA was also isolated and prepared for sequencing from the same SQ20B cells grown *in vitro* under hypoxic and normoxic conditions. Cells were grown in 0.5% oxygen for 16h because this falls within the range of oxygen levels observed in hypoxic tumors and accounts for prolonged exposure to these conditions which occurs *in vivo*. This approach allowed us to deeply investigate transcriptome changes due to hypoxic stress alone, without the influence of additional cellular stresses such as nutrient deprivation or changes in pH, which occur within the tumor microenvironment in an *in vivo* setting. The following data represent the first comparative hypoxic transcriptome study at nucleotide resolution of HNC *in vivo* and *in vitro*.

Results

Changes in individual mRNA isoform expression patterns represent an additional layer of hypoxia-regulated gene expression

The sequencing data were aligned and transcripts were assembled using the RefSeq human genome version 19 reference; expression levels were quantified as fragments per kilobase of transcript per million mapped reads (FPKM) for known RefSeq transcripts (72, 73). To achieve a finer resolution of hypoxia-regulated changes in expression, individual mRNA transcripts were examined to define gene expression at an isoform level. For the *in vitro* dataset, 18,915 individual mRNA transcripts were expressed (FPKM ≥ 0.5) in either normoxic or hypoxic SQ20B cells. For the *in vivo* samples, there were 18,573 transcripts detected (mean FPKM ≥0.5). Of the total 16,277 transcripts detected in both the *in vivo* and *in vitro* datasets, there was a modest positive correlation

in hypoxia-mediated changes in expression (Spearman correlation ρ=0.49, transcripts filtered for differentially expressed in hypoxia vs. normoxia P<0.05, FDR< 5%).

The *in vitro* data revealed 2,617 hypoxia-responsive transcripts (P<0.05, FDR< 5%). Fold change in expression in hypoxia compared to normoxia ranged from -10.4 to 76.1. A similar trend was observed for the *in vivo* study which contained 2,263 transcripts that significantly changed expression under hypoxia (P<0.05, FDR<5%), with fold-change in expression values ranging from -52.1 to 45.8. Hypoxia-induced transcripts (represented by 628 *in vivo* and 1,142 *in vitro*) were the subset of mRNAs which exhibited the strongest correlation (Spearman correlation ρ=0.501, Fig 2.1), with 268 transcripts representing 262 unique genes significantly induced in both datasets. The expression profiles are consistent with genes previously reported to be regulated by cellular oxygen levels. Gene ontology analysis confirmed that transcripts commonly induced in both datasets are significantly enriched for hypoxia-responsive genes and genes involved in glycolysis, and HIF-1α target genes.

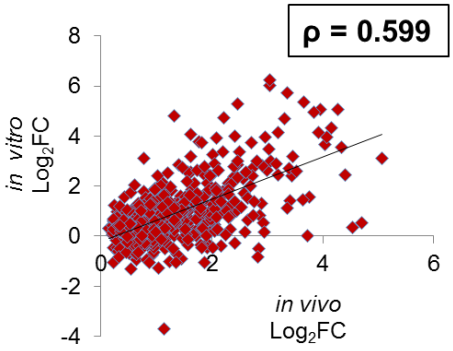

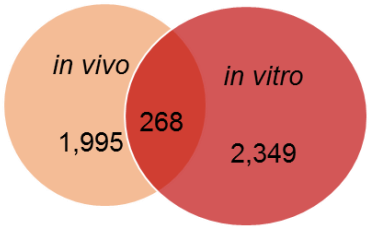

Ontology Term	Representative genes	P-value
response to hypoxia	*ADM, ALDOC, BNIP3, CA9, VEGFA*	6.2×10^{-07}
glucose, hexose metabolic process	*ALDOA, GPI, HK2, PDK1, PFKFP*	4.0×10^{-06}

Figure 2.1: Comparison of hypoxia-induced mRNAs from *in vivo* and *in vitro* studies of head and neck cancer cells. For correlation, mRNAs identified as significantly induced in hypoxic compared to normoxic cells (P<0.05 for at least one study). Log_2 fold-change in expression is plotted, with corresponding Spearman ranked correlation coefficient. Venn diagrams represent the number of mRNAs significantly induced for each dataset (P<0.05). Top gene ontology terms with examples listed below (DAVID Gene Ontology, FDR<%5).

Many targets of HIF-1α were among the most induced transcripts, including *VEGFA*, *ADM* and *CA9*. Select HIF-1α targets were chosen for validation and showed similar induction patterns for both RNA-seq and RT-qPCR methods (Fig 2.2).

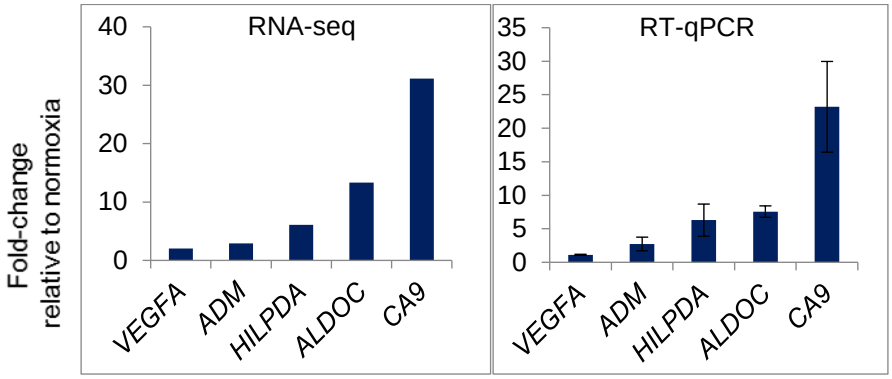

Figure 2.2: RT-qPCR validation of select HIF-1α target genes. For each set of graphs, RNAseq data shown to the left and corresponding RT-qPCR shown at right (average of three, independent experiments +/- S.E.M.) for SQ20B cells in normoxia or 0.5% O_2 for 16h.

There were similar numbers of repressed transcripts in hypoxic samples from each study, including 1,475 transcripts from 1,454 unique genes from the *in vitro* data, and 1,635 transcripts from 1,570 genes in the *in vivo* study. Altogether, the correlation between the two studies for this set of transcripts was modestly weaker compared to hypoxia-induced genes, (Spearman correlation ρ=0.262, Fig 2.3) even though the overlap included a larger number of transcripts than hypoxia-induced genes.

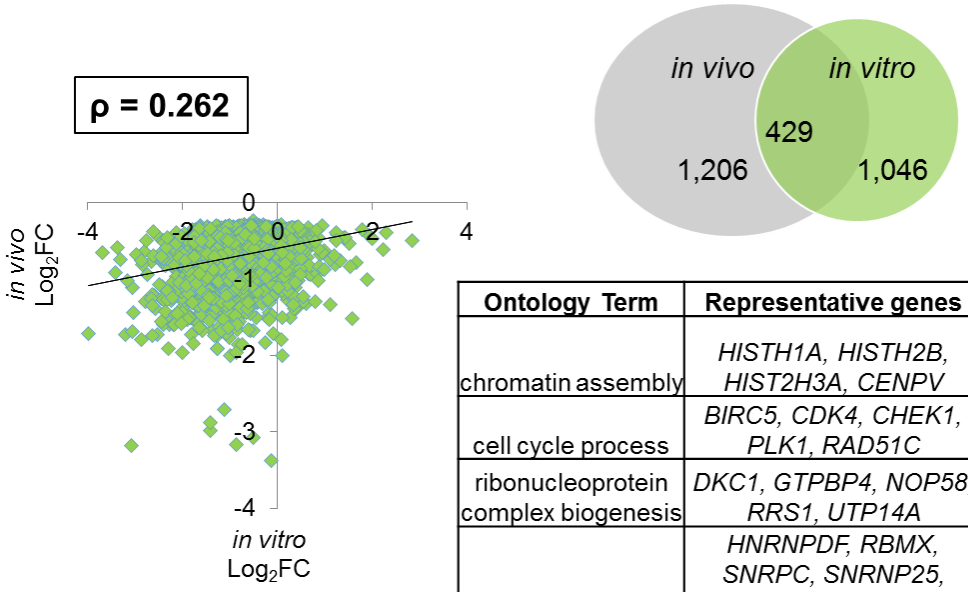

Ontology Term	Representative genes	P-value
chromatin assembly	*HISTH1A, HISTH2B, HIST2H3A, CENPV*	1.4 x10^{-16}
cell cycle process	*BIRC5, CDK4, CHEK1, PLK1, RAD51C*	2.8 x10^{-11}
ribonucleoprotein complex biogenesis	*DKC1, GTPBP4, NOP58, RRS1, UTP14A*	7.1 x10^{-08}
RNA processing	*HNRNPDF, RBMX, SNRPC, SNRNP25, SRSF3*	2.6 x10^{-07}

Figure 2.3: Comparison of hypoxia-repressed mRNAs from *in vivo* and *in vitro* studies of head and neck cancer cells. For correlation, mRNAs identified as significantly repressed in hypoxic compared to normoxic cells (P<0.05 for at least one study). Log_2 fold-change in expression is plotted, with corresponding Spearman ranked correlation coefficient. Venn diagrams represent the number of mRNAs significantly repressed for each dataset (P<0.05). Top gene ontology terms with examples listed below (DAVID Gene Ontology, FDR<%5).

I observed mRNAs downregulated in both the *in vivo* and *in vitro* samples to play roles in several pathways involving DNA-protein interactions, including chromatin organization, nucleosome assembly, cell cycle and RNA processing (Fig 2.3). Key hypoxia-responsive transcripts in these categories encode histone proteins, core RNA binding proteins including *HNRNPF*, *SRSF3* and *SNRPC*, and various factors that influence translation such as *DKC1*, *NOP10*, *RRS1* and *UTP6*. Select highly induced and repressed transcripts were validated by RT-qPCR (Fig 2.4).

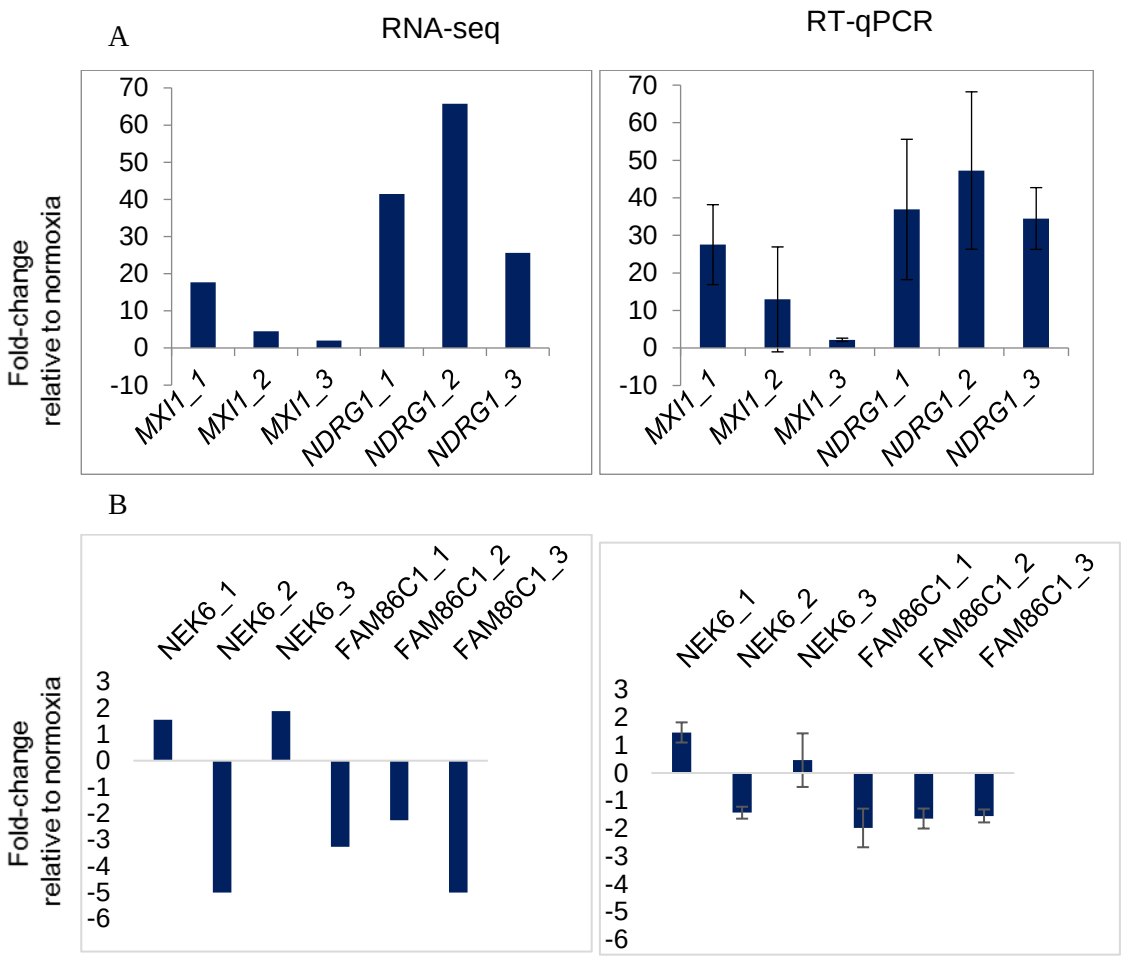

Figure 2.4: RT-qPCR validation of hypoxia-induced changes in mRNA expression detected by RNAseq. A: Induced isoforms, with isoform 1,2, or 3 designated with number following gene symbol. B: Repressed isoforms, with isoform 1,2 or 3 labeled. For each set of graphs, RNAseq data shown to the left and corresponding RT-qPCR shown at right (average of three, independent experiments +/- S.E.M.) for SQ20B cells in normoxia or 0.5% O_2 for 16h.

These data revealed previously unreported patterns of differential isoform expression in genes that are established to be stress-responsive at the total gene level.

By examining individual mRNA transcript-level differences, I observed differences in the predicted biological functions of these isoforms as well. For example, isoform 1 of the gene MAX-interactor 1 (*MXI1*) was preferentially induced under hypoxia compared to isoform 3 (Fig 2.4). Additionally, there were functional differences between the isoforms of *MXI1*, which differ at the amino-terminus thereby altering its ability to antagonize N-Myc activity and impact cell proliferation (74, 75). Hypoxia selectively induced the transcript which is translated into the shortest protein isoform. This isoform lacks 46 amino acids at the N-terminus compared to isoform 3 and is more than approximately 10kDa smaller than the full length MXI1 protein. Likewise, three isoforms of *NDRG1* were induced by hypoxia, but isoform 2 exhibited the strongest induction (Fig 2.4). Compared to the other two isoforms of *NDRG1*, isoform 2 lacks the proteolytic cleavage site at Cys49-Gly50 due to an alternative transcription start site, resulting in 66 fewer amino acids at the N-terminus. The isoforms of two additional genes, *NEK6* and *FAM86C1*, were validated as being selectively repressed under hypoxic conditions (Fig 2.4).

Analysis of genes expressing more than one mRNA isoform identified previously undescribed hypoxia-responsive genes

In human cells, nearly all multi-exon genes are affected by alternative splicing and may be expressed as more than one mRNA transcript variant. Alternative splicing can be controlled in a tissue or cell-specific manner, but is also regulated through cell signaling pathways in response to physiologic or extrinsic stresses. To determine the influence of hypoxic stress on alterations in mRNA splicing, I first examined those genes expressed

as multiple mRNA transcripts. Approximately 33% of the genes expressed in the *in vivo* RNA-seq data (6122 of 18745) were expressed as more than one transcript. Similarly, 37% of genes observed in the *in vitro* study (5420 of 14651) were expressed as more than one mRNA variant.

Instead of measuring total gene expression levels, the resolution of our data allowed us to define hypoxia-responsive genes as any gene with one or more individual mRNA transcript differentially expressed under hypoxia compared to normoxia ($P<0.05$, FDR<5%). Using these criteria, of the genes that expressed more than 1 isoform, 1,216 (*in vitro*) and 2,347 (*in vivo*) contained at least one differentially expressed isoform. Nearly 75% of these genes would not have been identified as regulated by hypoxia without studying changes in individual transcript expression; only 331 of 1,216 genes (*in vitro*) and 521 of 2,347 (*in vivo*) were identified in literature reports from traditional microarray studies, including a curated database of over 2,000 genes reported as regulated under conditions of low oxygen (76).

Because variation in expression of several mRNA transcripts of the same gene could be masked when analyzing total gene expression changes (measured as the sum of all transcripts), I next searched for genes with one or more differentially expressed isoform that were not detected as hypoxia-responsive at the total gene level. For the *in vitro* data, there were 61 of 1,216 genes with at least one differentially expressed transcript which were not detected as differentially expressed at the total gene level in our analysis. Of these 61, only 11 genes were previously reported as differentially expressed in conditions of low oxygen (*in vitro*) confirming that these data led to the discovery of 50 previously unreported hypoxia-responsive genes by measuring individual mRNA levels as opposed to total gene levels. These 50 genes were functionally

enriched for roles in protein localization (*SEC24B*, *ARL17A*, *PLEKHA8*, *MLPH*, *STXBP5*, *MON2*, and *EXOC1*), MAPKK signaling (*MAP4K3*, *DUSP22*, and *MAP3K13*) and regulation of RNA metabolism (*ZNF519*, *JDP2*, *CTBP2*, *ZNF248*, *RBM5*, *NFAT5*, *CREB3L2*, *SMARCA1* and *ZFHX3*) (DAVID Gene Ontology, P<0.05). The same analysis was carried out for the *in vivo* dataset, and filtered for genes commonly found to be hypoxia-specific in the *in vitro* set. This revealed 7 genes previously undescribed as hypoxia-responsive which occurred in both the *in vitro* and *in vivo* datasets. These genes included those predicted to carry out roles in protein localization (i.e. *PLEKHA8*, *MLPH*) and RNA metabolism (*ZNF519*), and several other genes such as the *SSH1* phosphatase involved in cell migration (77), the *IP6K2* kinase linked to regulation of cell death (78), a transcription factor of inflammatory genes (*NFAT5*) and the *C16orf40* gene of unknown function.

Determining the contribution of HIF-1α & hypoxia-response element (HRE) sequences in regulating differential isoform expression

Because many hypoxia-induced changes in gene expression are influenced by HIF transcription factor binding at conserved hypoxia-responsive element (HRE) sequences, I carried out a meta-analysis to look at HIF-1α binding patterns (experimentally validated by ChIP-seq (79)) and occurrence of HRE sequences at genes with differential isoform expression under hypoxia. For in the *in vitro* genes, approximately 4.7% genes with a hypoxia-responsive mRNA contain an HRE sequence reported to be bound by HIF-1α. If I only considered those genes which expressed more than one transcript and were affected by differential isoform expression, only approximately 5.3% of these genes

contain HRE sequences or have previously reported HIF-1α binding. For the genes with a hypoxia-responsive mRNA *in vivo* data, approximately 5.1% genes contain an HRE sequence or HIF-1α binding site. The proportion of genes which expressed more than one transcript and contain either an HRE or HIF-1α binding site was the same (5.0%). Altogether, these data suggest alternative splicing and differential isoform expression of hypoxia-responsive genes are regulated in an HRE-independent manner and that HIF-1α is not a major contributor to global changes in splicing under hypoxia. This is consistent with other reports, because although mRNA splicing occurs co-transcriptionally, regulation of transcription and mRNA splicing are distinct processes which can impact different subsets of genes (80).

Key regulators of splicing catalysis are repressed under hypoxia

Intriguingly, there was an enrichment for hypoxia-responsive genes involved in RNA processing, transcription elongation and RNA polymerase II regulation ($P<0.05$, DAVID Gene Ontology Analysis (81)) and an overall repression of many regulators of mRNA splicing (Figs 2.3, 2.5). This included many RNA binding proteins such as poly(A) binding proteins, RBM (RNA binding motif) genes, and major splicing factors including the serine-arginine rich factor *SRSF1* and several SF3B family members. Strikingly, the expression levels of these pathways were regulated similarly in both datasets (Fig 2.5). Upon closer examination of genes involved in splicing catalysis, I observed a marked repression of genes involved in nearly all major steps of splicing, including spliceosomal assembly, exon definition and intron lariat removal (Fig 2.6).

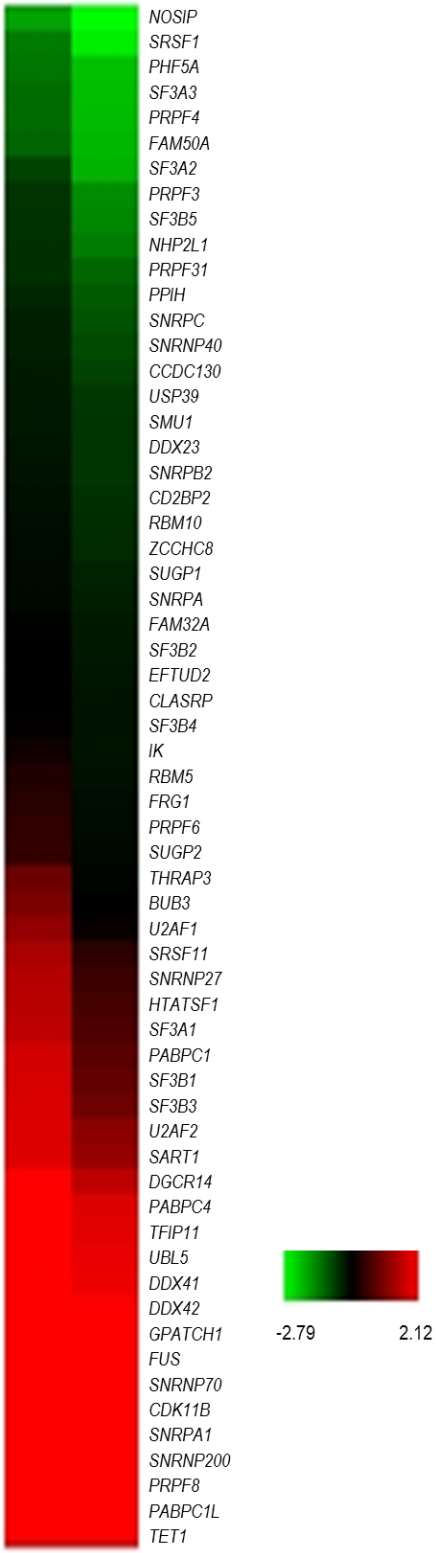

Figure 2.5: Hypoxia alters expression of RNA processing and splicing factors. Heatmap of expression fold-changes for RNA processing genes significantly altered in hypoxic cells ($P<0.05$ for at least one dataset).

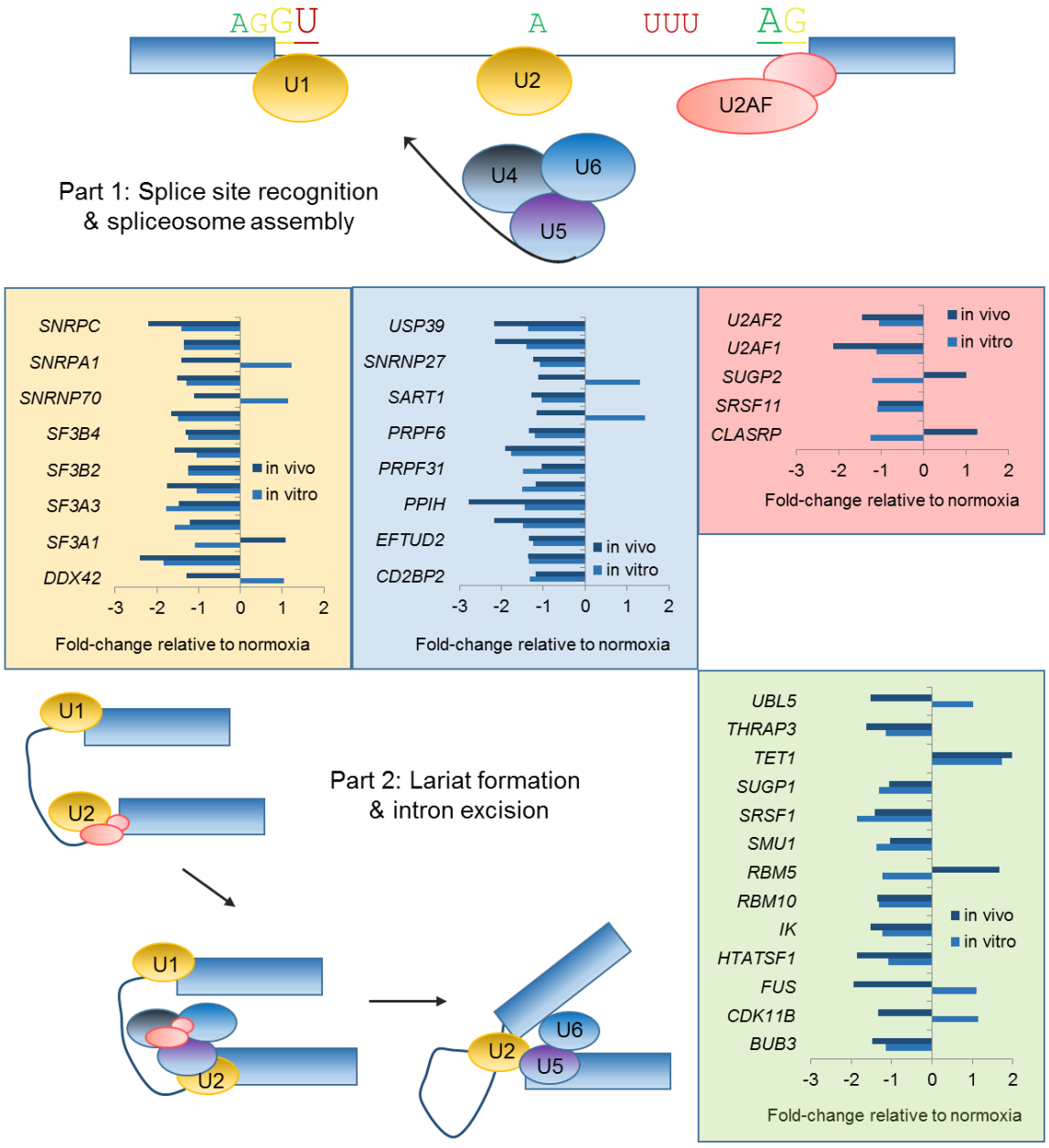

Figure 2.6: RNA-Seq expression data for *in vivo* & *in vitro* study of hypoxic head and neck cancer cells reveals downregulation of genes involved in splicing catalysis. Top panels describe the initial steps including binding at conserved splice sites (at the intron:exon junction) and branchpoint sequences (depicted in the intron). Lower panel includes genes involved in the regulation of the final steps for intron removal. List of eukaryotic genes involved in catalysis steps based on summary described from previous studies (3).

Discussion

Next-generation sequencing analyses of hypoxic tumor microenvironments yield greater resolution of transcriptome changes. The results from these transcriptome studies provided an in-depth look into changes in mRNA levels and patterns of differential mRNA isoform at a resolution that has yet to be described. The similarities observed in the regulation of hypoxia-responsive genes in the *in vivo* and *in vitro* models of HNC further establish EF5-labeling coupled with LCM as a validated technique for the specific gene expression profiling of hypoxic cells within the tumor microenvironment. These data also highlight the advantages of high-resolution RNA-sequencing data in studying stress-responsive gene expression programs, as I could identify genes previously unreported as hypoxia-responsive. Additionally, genes established as hypoxia-responsive were shown to contain complex patterns of differential isoform expression which may provide clues to hypoxia-specific isoforms which carry out distinct functions. For example, *NDRG1* encodes a stress-responsive cytoplasmic protein that activates p53-mediated apoptosis and can suppress metastasis; hypoxia-induced alternative splicing in this gene leads to expression of an isoform lacking a proteolytic cleavage site, which would likely alter the function of the resulting protein (82). Similarly, isoform 2 of the gene *NEK6* is selectively repressed compared to other isoforms of *NEK6* (Fig 2.4). This gene encodes a serine-threonine kinase and cooperates with HIF-1α to promote anchorage-independent growth in ovarian cancer cells; its expression is correlated with ovarian cancer aggressiveness (83).

While my data did not identify HIF-1α as a major contributor of hypoxia-mediated changes in patterns of isoform expression, it does influence splicing of portion of genes transcriptionally induced by HIF-1α. Interestingly, 6 of the 7 putative HIF-1α binding sites

that occur nearby the first two exons of *NEK6*, which is where isoform 2 differs compared to other transcripts of *NEK6*. Likewise, splicing of *MXI1* is directly influenced by HIF-binding, which impacts alternative promoter usage in this gene (84). Splicing is differentially regulated in cancer due to a number of biological alterations, including mutations in spliceosomal genes or mutations in specific splice sites of genes, but also due to changes in expression of key signaling networks. Hypoxia is a major stress in the tumor microenvironment that leads to widespread changes in gene expression; here we observed significant repression of genes involved in pathways known to regulate the RNA processing and splicing (Figs 2.3, 2.5, 2.6). Because many regulators of splicing catalysis were repressed in hypoxic cells, I hypothesize that regulated changes in mRNA splicing may represent an additional layer of gene expression control under hypoxia. In order to deeply characterize hypoxia-regulated differences in alternative splicing and to investigate the resulting biological implications, I next carried out an exon-level analysis of changes in mRNA structure using the mixture of isoforms (MISO) platform (85). Since the *in vitro* datasets had nearly twice as many uniquely aligned reads than the *in vivo* dataset and the additional advantage of paired-end sequencing, I exclusively used the *in vitro* RNA-seq data for this analysis. This provided me with an ideal dataset for specifically and confidently measuring expression at splice junctions to detect rare and lowly expressed alternatively spliced forms under hypoxia. These data will be the basis of Chapter 3, and importantly led to the discovery of a unique alternatively spliced isoform of the eukaryotic translation initiation factor, *EIF2B5*, which we show is selectively induced under hypoxia and acts in opposition to the full-length isoform to inhibit protein synthesis. Altogether, these transcriptome studies provide strong support for the inclusion and deep investigation of alternatively spliced transcripts when

evaluating cellular responses to stress, such as those that occur within the tumor microenvironment.

CHAPTER 3

Transcriptome analysis of hypoxic cancer cells uncovers intron retention in *EIF2B5* as a mechanism to inhibit translation

The work in this chapter contributes to a manuscript of the same title currently under revision in *PLOS* Biology.

Introduction

Reduced availability of oxygen, or hypoxia, is a major feature of solid tumors that contributes to metastasis and resistance to therapy (86). Tumor hypoxia occurs due to several physiological factors, such as limited diffusion of oxygen and irregular vascular structure (87). While oxygen levels can be measured directly in tumors, there is an immediate need to develop non-invasive clinical markers of hypoxic burden in tumors. Molecular imaging markers such as pimonidazole and fluorescence-based compounds (88-90) have been developed and refined to specifically label hypoxic tumors, which allow for specific interrogation of hypoxic gene expression programs within the tumor microenvironment (25). Hypoxia-mediated changes in expression can be dynamic and robust, impacting pathways critical to tumor development and survival, such as angiogenesis, metabolism and macromolecular synthesis (9, 91). Consequently, there is a nearly universal negative correlation between the level of hypoxia in tumors and overall survival in patients of many solid cancers, including head and neck squamous cell carcinoma (HNSC) (19). As such, hypoxia “metagene” expression signatures have been successfully implemented as a surrogate method to classify tumor hypoxia for HNSC and other solid malignancies, including breast and prostate cancer (20, 21).

Hypoxic stress influences processing and translation of mRNAs by regulating the levels and activity of diverse factors including Hypoxia-Inducible transcription Factors (HIFs), small non-coding RNAs and miRNAs and RNA binding proteins (RBPs) (33-35). For example, RBPs such as HuR and PTB, bind to and regulate the stability and localization of key regulators of hypoxic response such as HIF1α (36, 37) and miRNA-199a (38). Several kinases known to phosphorylate major RBPs and splicing factors are also

hypoxia-responsive (54), and alternative splicing of select target genes of HIF1α has been reported in hypoxic cells (50). Likewise, expression of non-coding mRNA isoforms are induced under hypoxia in part due to changes in splicing (51). Several splicing factors, including SF3B1, are upregulated in a HIF1α-dependent manner under physiological conditions of hypoxia in cardiac myocytes (55); however, it remains unclear precisely how mRNA splicing is regulated during periods of oxygen deprivation in cancer cells and what the resulting biological implications are. Intriguingly, regulation of splicing is frequently altered in cancer and is affected by the same signaling pathways that are differentially regulated in hypoxic tumor microenvironments (53). Many solid cancers affected by hypoxia display widespread alterations in splicing (66).

While splicing of specific genes has been shown to be dependent on the activity of HIF1α, I hypothesized that hypoxia-mediated changes on the RNA processing and transcription machinery could lead to extensive differences in mRNA splicing. Hypoxia was identified to induce phosphorylation of the C-terminal domain of RNA polymerase II (RNAPII), which led to enhanced binding of co-factors and increased control of transcriptional activation of HIF target genes (92).

Additional findings support that changes in the activity and rate of transcription elongation play a key role in the maturation and processing of mRNAs under hypoxia. Under hypoxia, there are fewer changes in RNAPII binding near gene promoters, but instead an increased accumulation of RNAPII observed along gene bodies (93); differences in transcription elongation are known to impact regulation of co-transcriptional splicing (94-96). Therefore, to better understand the link between hypoxia-mediated changes to mRNA regulation and to investigate the biological role of alternative splicing in response to hypoxia in cancer, I deeply sequenced the mRNA of hypoxic and normoxic HNSC SQ20B cells.

The data led to the identification of more than 1,000 transcripts affected by alternative splicing under hypoxia and revealed three types of mRNA splicing as specifically enriched, including an increase in retained introns in hypoxia compared to normoxia. Strikingly, for more than 90% of genes in this category, hypoxia increased the occurrence of retained introns relative to normoxia, which is a phenomenon also observed in 16 cancer types, including head and neck, colon, breast and lung cancers (66). Notably, I discovered a unique retained intron in the master regulator of translation initiation, *EIF2B5*. More importantly, this retained intron is expressed in multiple cancers affected by hypoxic fractions and is overexpressed in HNSC tumors relative to normal tissues. Here I present compelling evidence hypoxia leads to retention of an intron in *EIF2B5* which creates a phylogenetically conserved premature termination codon. This alternate transcript results in a truncated protein isoform of eIF2Bε predicted to lack enzymatic guanine exchange factor (GEF) activity. Remarkably, I demonstrate that the resulting truncated isoform of eIF2Bε is induced under hypoxia, and provide data to show that this isoform acts in opposition to full length eIF2Bε to inhibit protein synthesis. Cellular adaptation to hypoxia entails adjusting key metabolic processes, such as translation, to low energy due to reduced availability of oxygen (49). Control of translation initiation specifically contributes to downregulation of protein synthesis under hypoxia, which occurs through phosphorylation of eIF2α by hypoxia-mediated induction of the integrated stress response (97). Here, I am the first to my knowledge to describe hypoxia-mediated induction of a dominant-negative isoform of eIF2Bε as a secondary method to inhibit translation in periods of acute or prolonged hypoxia. I further investigated how splicing of *EIF2B5* is controlled, and uncovered contributions of several factors, including a weak splice site at the intron:exon junction, hypoxia-induced expression and binding of SRSF3, and an accumulation of RNAPII specifically at the

retained intron.

Results

Hypoxia-mediated changes in transcript-level expression

The transcriptomes of normoxic and hypoxic SQ20B cells (maintained in 0.5% O_2 for 16h) were compared to identify expression differences at an individual mRNA transcript level. The RefSeq hg19 reference comprised of 46,017 transcript models was used for annotation. Of the 24,812 transcripts expressed in SQ20B cells, I detected 3,114 that significantly changed expression in hypoxia compared to normoxia (P< 0.05, FDR< 5%, FPKM≥ 0.5). In total, 1,519 transcripts representing 1,473 genes were induced and 1,595 transcripts expressed from 1,563 genes were repressed (FDR< 5%). Pathway-based analysis identified “cell adhesion”, “response to hypoxia” and “metabolism” among the most enriched categories for hypoxia-induced transcripts (P<0.01, DAVID GO(81)). Induction of select HIF1α target genes was validated by qPCR (Fig 2.2). Repressed genes were involved in regulating processing, stability and translation of RNAs, with “ribosome biogenesis”, “nucleosome organization” and “RNA splicing” as highly significant ontology groups (P<0.01). This included core regulators of splicing, such as the major splicing factor *SF1*, serine-arginine splicing factors (*SRSF1*, *SRSF3* and *SRSF7), SF3* genes, and many translation initiation factors, including *EIF2B* family members, *EIF5* and *EIF6*. Notably, a closer examination of genes involved in regulation of mRNA transcription, translation and processing, revealed that the clear majority of these genes were repressed under hypoxia (Fig 3.1A).

Variation in expression of individual transcripts of the same gene by hypoxia could be masked when analyzing expression changes at the total gene level; therefore, I next

used levels of individual isoforms to classify genes as hypoxia-responsive (defined as a gene with one or more individual transcript detected as significantly induced or repressed, P<0.05, FDR< 5%). This analysis uncovered 50 additional genes which may not yet be reported as hypoxia-regulated, including genes known to mediate protein localization, (*SEC24B*, *ARL17A*, *PLEKHA8*, *MLPH*, *STXBP5*, *MON2*, and *EXOC1*), MAPKK signaling pathway, (*MAP4K3*, *DUSP22*, and *MAP3K13)* and key regulators of RNA metabolism, (*ZNF519*, *JDP2*, *CTBP2*, *ZNF248*, *RBM5*, *NFAT5*, *CREB3L2*, *SMARCA1* and *ZFHX3)*. Consistent with the finding that transcript-level changes comprise an additional layer of hypoxia-regulated expression changes, only approximately 3% of genes which expressed multiple isoforms in SQ20B cells have been reported to be transcriptionally controlled by HIF binding at hypoxia-responsive elements (HRE) (98), suggesting an HRE-independent mode of regulation. This is not surprising, as regulation of transcription and mRNA splicing are observed to be distinct processes which impact different subsets of genes (80).

Next, I focused on those genes that expressed more than one transcript in SQ20B cells to assess changes in patterns of isoform expression. Of the 5,418 genes identified to express >1 transcript, 937 of these genes showed hypoxia-induced changes in expression of 1,015 transcripts (P< 0.05, FDR<5%). Most these genes contained a single hypoxia-responsive isoform; only 8% of genes that expressed multiple transcripts showed more than one isoform as significantly changed under hypoxia.

Functional classification of changes in alternative splicing

I reasoned that hypoxia-responsive isoforms predicted to carry out different functions than isoforms expressed in normoxia would be the most biologically impactful changes which warranted further study. Therefore, I used the program MISO (85) to carry out an additional exon-level approach to identify changes in gene structure based on eight annotated categories of alternative splicing. Hypoxia led to a change in expression for 1,103 alternatively spliced loci representing 819 unique genes (Fig 3.1B, ΔPsi >10%, Bayes Factor >20). Notably, there was a significant comparative enrichment for hypoxia-induced changes in three specific event types: expression of alternate last exons (ALE), retained introns (RI) and tandem 3' UTRs (Fig 3.1B). For the genes in these three splicing categories, gene ontology revealed processes central to hypoxic adaptation as significantly enriched, including "cellular protein metabolism", "programmed cell death" and "gene expression" (DAVID GO, P<0.05, Fig 3.1C). Remarkably, nearly 90% of the genes in the RI category displayed increased retention of introns in hypoxic compared to normoxic cells (Fig 3.1D). Among these genes was *ANKZF1,* a gene implicated in

Figure 3.1 (Next page)- Classification of alternatively spliced mRNAs in hypoxic SQ20B cells. A: Heatmap of RNA processing and splicing factors differentially expressed in hypoxia compared to normoxia (Fold-changes shown, FDR<5%). B: To left, plot depicts number of events detected (blue) compared to events with significantly different expression in hypoxic compared to normoxic cells (red) (Bayes Factor ≥20, $\Delta\Psi$ > 10%; SE = skipped exon, RI = retained intron, A5SS = alternative 5' splice site, A3SS = alternative 3' splice site, AFE = alternative first exon, ALE = alternative last exon, MXE = mutually exclusive exon, TUTR = tandem 3' untranslated region). Specific enrichment for changes in three event types are starred: ALE, RI, TUTR (***P< 0.001, 2-sample test for equality of proportions). To right of graph, exon models of the types of splicing assessed by MISO analysis. C: Gene ontology figure representing functional enrichment for hypoxia-induced changes in ALE, RI and TUTR categories. D: Percent spliced in (Psi) values plotted with hypoxia samples (red) overlaid against corresponding normoxic Psi values (blue). E: PCR validation of intron retention events in *EIF2B5* and *ANKZF1* genes. Diagrams to right of gel images of PCR products depict exons as solid blue and introns as striped rectangles.

mitochondrial and endoplasmic reticulum-associated protein degradation (99, 100), the translation initiation factor *EIF2B5*, *TGFB1* and the metionyl-TRNA synthetase, *MARS*. The retained introns in these genes were validated by PCR using primers spanning the intron junction and cDNA prepared from oligo-dT selected mRNA (Fig 3.1E).

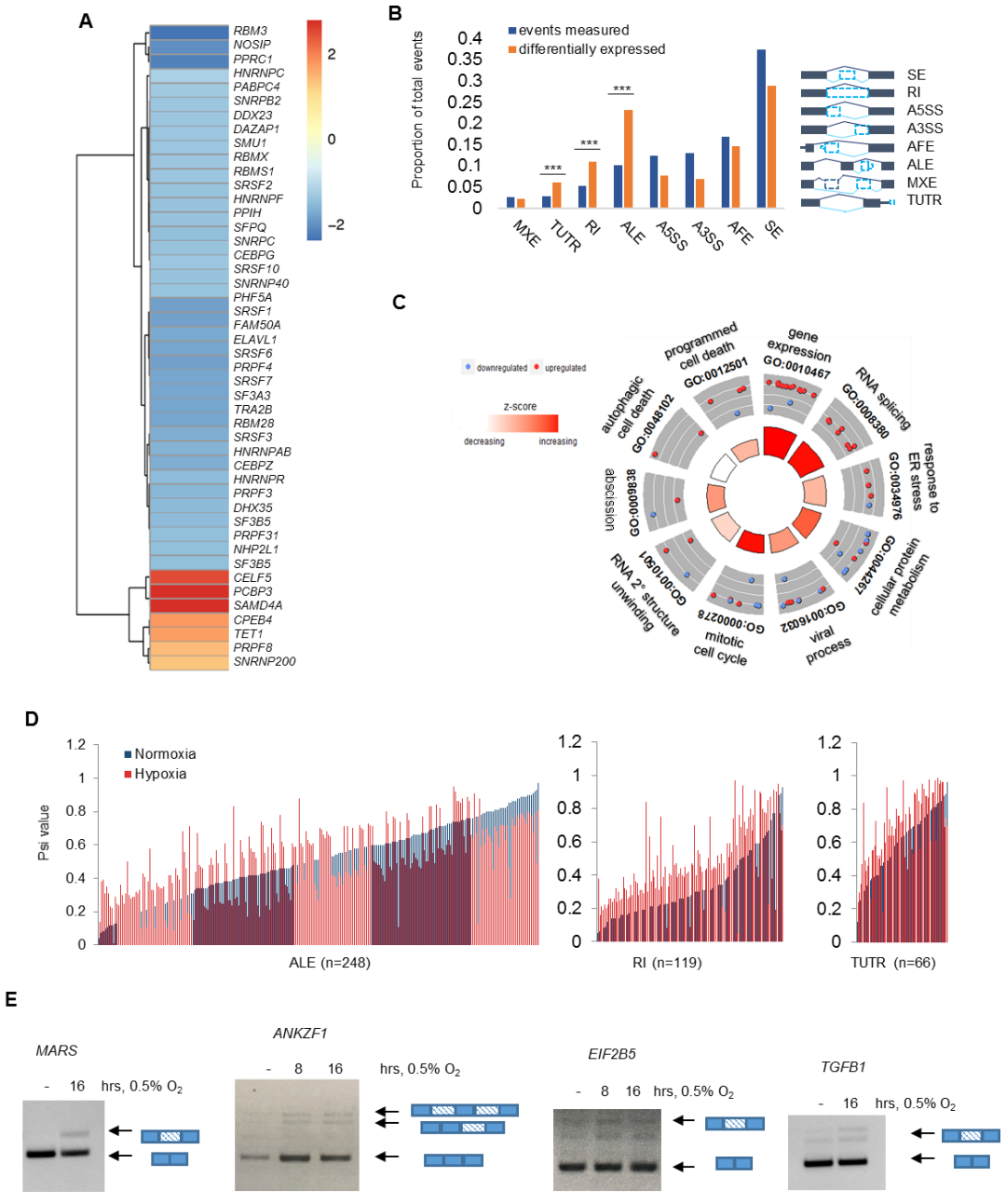

Strikingly, *EIF2B5* stood out as the strongest candidate for further functional studies for several reasons: (a) hypoxia led to a >40% increase in retention of intron 12 in a background of an overall 2-fold decrease in total expression of *EIF2B5* ($\Delta\Psi$ = 0.44, Bayes Factor >20), (b) the retention occurred specifically at a single locus of *EIF2B5* and (c) retention of intron 12 creates a premature termination codon (PTC) that remains in frame with the coding sequence (Fig 3.2). The genomic locus around the PTC is highly conserved even among lower organisms. Intriguingly, this stop codon is part of the 5' splice site consensus sequence "GURAGU" where URA can be either UAA or UGA (both of which would create a stop codon). This suggests a strong evolutionary pressure to

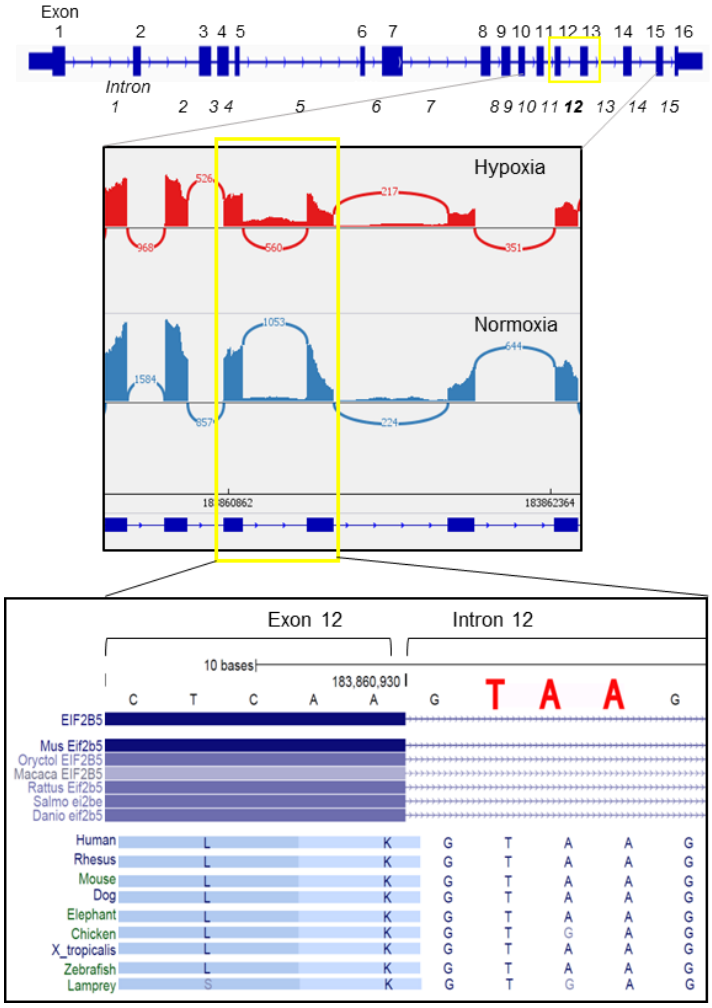

Figure 3.2: Hypoxia promotes intron retention in *EIF2B5* and insertion of an evolutionarily conserved premature termination codon. Upper: Gene model of *EIF2B5*, with sashimi plot of normalized RNA-seq reads for representative matched hypoxia and normoxia samples (plot created using Integrative Genome Viewer). Lower: UCSC Genome Browser Vertebrate Conservation track reveals a conserved stop codon (TAA or TGA), which remains in frame upon retention of intron 12.

preserve an early termination precisely at this location where inclusion of the PTC may be influenced through regulation of splice site choice.

A deeper analysis of changes in splicing of *EIF2B5* was carried out to closely examine inclusion of intron 12 and to validate the occurrence of this retained intron using another method; the software package MAJIQ (101) was used to assess local splicing variation in *EIF2B5* for annotated and *de novo* splice events. A hypoxia-induced increase in expression of intron 12 was confirmed using this approach (Fig 3.3) but additional sites of local splicing variation did not show significant (>20%) hypoxia-influenced changes.

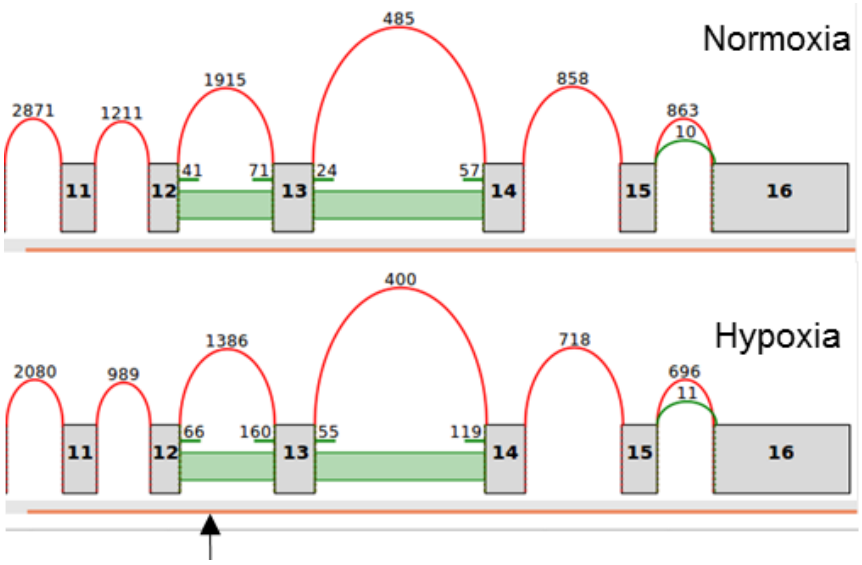

Figure 3.3: Additional analysis of *EIF2B5* splice junction reads. A: Splice graph of 3' end of EIF2B5 displaying splice junction reads for all normoxia and hypoxia samples, with arrow signifying intron 12 (created using MAJIQ/VOILA). RNAseq expression data are reported as mean, normalized read counts at each junction for all 4 normoxia and 4 hypoxia biological replicates.

Retention of intron 12 in *EIF2B5* is observed in tumors and leads to a truncated protein isoform

Increased expression of *EIF2B5*_intron12 was further confirmed by qPCR using intron-specific primers in a reaction with cDNA prepared from oligo-dT selected mRNA (Fig 3.4A). To confirm expression of *EIF2B5*_intron 12 in additional datasets and assess its levels in patient samples, The Cancer Genome Atlas (TCGA) was analyzed for expression of intron 12 in solid tumors known to be affected by hypoxic fractions (17, 102, 103). Expression of *EIF2B5*_intron12 was detected in samples derived from numerous solid tumors (Fig 3.4B). Even though the TCGA samples were not specifically sorted or selected according to levels of tumor hypoxia, the RNA-seq data collected from solid tumor samples will include hypoxic regions of the tumor tissue, while normal tissue samples will not contain as many hypoxic cells. Therefore, I predicted that levels of intron 12 would be higher in tumor relative to normal tissue. Indeed, we observed significantly increased expression of intron 12 in HNSC samples compared to matched, normal tissues (Fig 3.4C). This trend was even more apparent with patients in late-stage disease, with some individuals exhibiting nearly 8-fold increased expression of intron 12 compared to controls (Fig 3.4D). These data suggest hypoxia-induced retention of *EIF2B5* intron 12 may result in meaningful biological effects and encouraged us to test if this retained intron leads to a truncated protein isoform.

Computational analyses approximate up to 20-35% of alternatively spliced transcripts could contain PTCs and become targets of non-sense mediated decay (NMD) (43, 44), however in cases where NMD is inhibited, transcripts can be stabilized and subsequently translated into truncated proteins (45). Moreover, NMD surveillance typically recognizes stop codons as premature if the stop occurs more than 50 nucleotides upstream of a splice junction (42).

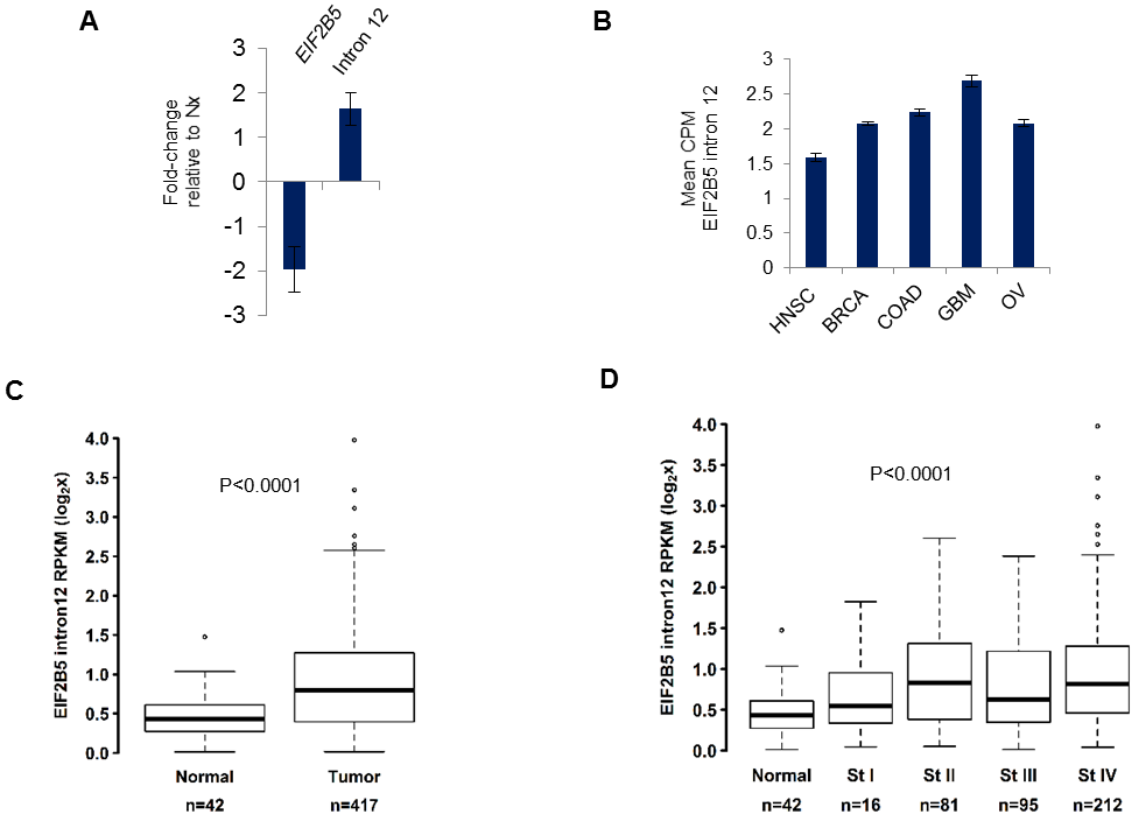

Figure 3.4: Expression of *EIF2B5* intron 12 is observed in tumors. A: Real time quantitative-PCR performed with isoform-specific primers in SQ20B cells. Data are presented as average of 3 independently conducted experiments, with error bars reported as s.e.m. B: Expression of intron 12 (chr3:183860931-183861231) was detected in level 1 RNA-seq data of various cancers examined from The Cancer Genome Atlas (CPM = read counts per million mapped reads); HNSC= head neck squamous cell carcinoma (n = 301), BRCA= breast cancer (n = 988), COAD= colon adenocarcinoma (n = 385), GBM= glioblastoma multiforme (n = 153), OV = serous ovarian cancer (n = 412). C: Expression of *EIF2B5*_intron12 was measured for head and neck cancer tumors compared to normal (P<0.0001). D: Expression of *EIF2B5*_intron12 was grouped by disease stage for the 417 head and neck tumor samples, and compared to available matched normal tissues ($P = 0.7 \times 10^{-4}$ Kruskal-Wallis non-parametric test).

Due to the unusual nature of this intron retention event and the role of hypoxia in suppressing nonsense-mediated decay (NMD) in an eIF2α phosphorylation-dependent manner (39), I predicted that this isoform would not be subject to NMD, but would rather be translated into a truncated protein (Fig 3.5A). Consistent with this hypothesis, the MAJIQ splicing analysis of *EIF2B5* revealed a 40-50% decrease in expression of remaining exons following intron 12 (Fig 3.3). These data support the notion that transcripts which retain intron 12 and the subsequent PTC would undergo read-through of intron 12 into intron 13, resulting in a reading frame for a truncated protein variant. Indeed, I observed induction of a 65kDa protein isoform of eIF2Bε under hypoxia, consistent with the predicted PTC inserted upon retention of intron 12 (Fig 3.5B). To further test whether this 65kDa protein was indeed a truncated isoform of eIF2Bε, I used siRNA to specifically target the entire *EIF2B5* gene or intron 12 alone. Using this approach, I observed a substantial reduction in the levels of the 65kDa isoform under both conditions (Fig 3.5C). I additionally observed hypoxia-induced expression of 65kDa eIF2Bε in the colorectal cancer cell line, RKO (Fig 3.5D), demonstrating that this is not a cell-line specific event. Moreover, UV-stress (Fig 3.5E), but not thapsigargin-induced ER stress, also led to induction of the truncated eIF2Bε, suggesting that expression of this isoform is induced by specific cell stresses. Furthermore, whole cell lysates were isolated from hypoxic SQ20B cells and proteins migrating at 80kDa and 65kDa were subjected to liquid-chromatography tandem mass-spectrometry. Peptides corresponding to eIF2Bε were detected in both the 80kDa and 65kDa size analytes.

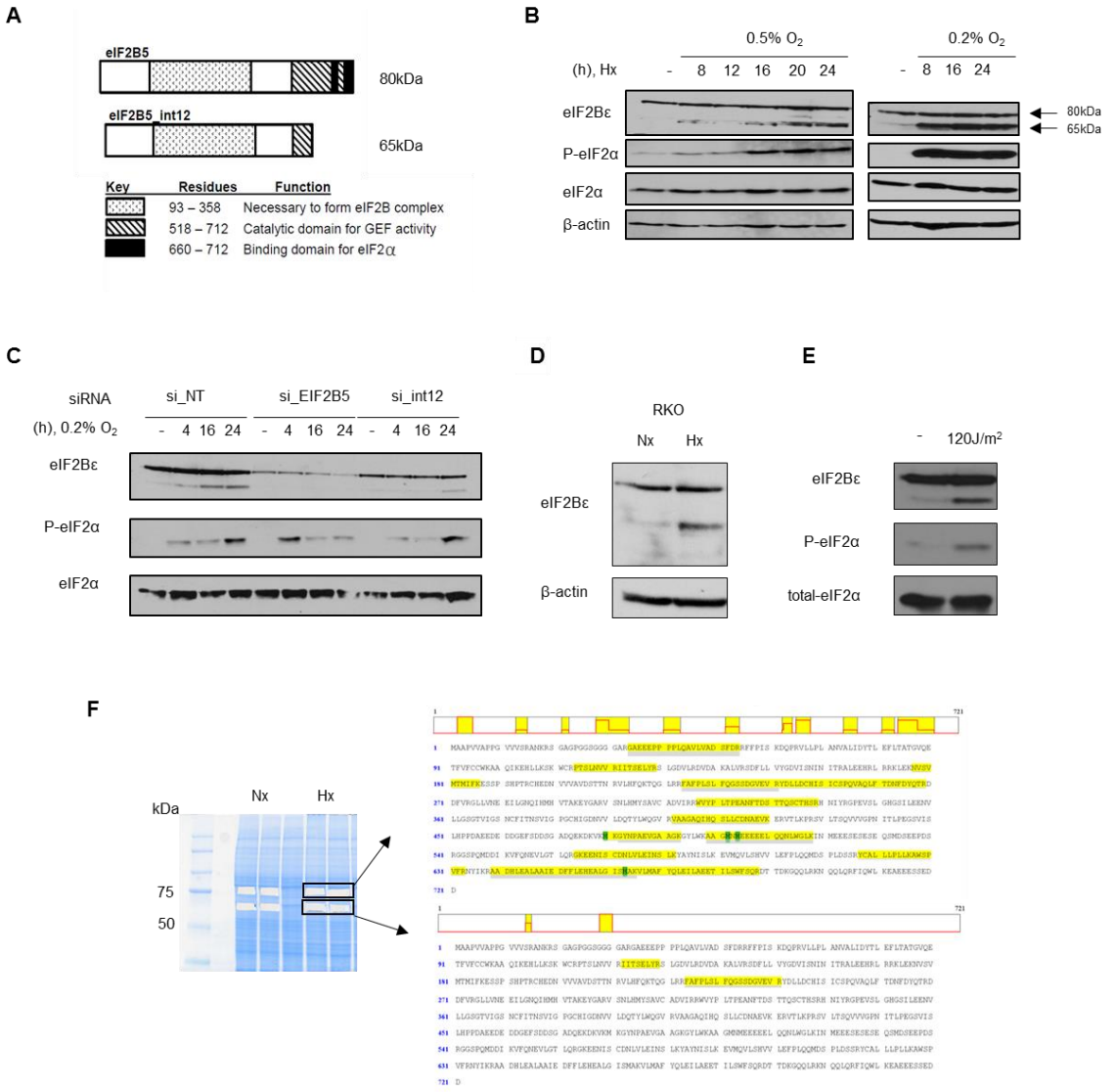

Figure 3.5: Retention of intron 12 leads to a 65kDa isoform of eIF2Bε. A: Protein model of observed isoforms of eIF2Bε. B: Immunoblot shows induction of a 65kDa isoform of eIF2Bε in SQ20B cells maintained for various periods in 0.5% or 0.2% O_2. C: Knock-down of eIF2Bε with siRNA targeting the whole gene or intron 12 reduces expression of the 65kDa isoform in normoxic and hypoxic (0.2% 0_2) SQ20B cells. NT = non-targeting control siRNA. D: Hypoxia (16h, 0.5% O_2) in a colon cancer cell line, RKO, leads to induction of 65kDa eIF2Bε. E: Immunoblot of SQ20B cells collected 4h after exposure to UV. F: Protein sequence of eIF2Bε with peptides identified from LC-MS/MS sequencing highlighted in yellow (shown to right). Analysis was carried out from gel-purified bands (shown left) corresponding to approximately 80kDa (top) and 65kDa (lower), which contained peptides of full-length eIF2Bε and a truncated isoform of eIF2Bε, respectively.

The peptides corresponding to the 65kDa-sized isoform of eIF2Bε were located near the N-terminus or middle of the eIF2Bε sequence, consistent with a C-terminal truncation (Fig 3.5F).

Finally, I carried out an experiment to test for the involvement of NMD in leading to expression of truncated eIF2Bε. Although NMD is known to be inhibited in conditions of oxygen deprivation, NMD and alternative splicing are coupled processes, which can lead to alternative PTC-containing transcripts which ultimately become targets of NMD (104). To rule out any major contribution of NMD in leading to expression of 65kDa eIF2Bε, we used siRNA to knock-down expression of UPF1. This experiment failed to produce an increase in expression of the truncated protein (Fig 3.6), further supporting the notion that this isoform occurs due to alternative splicing.

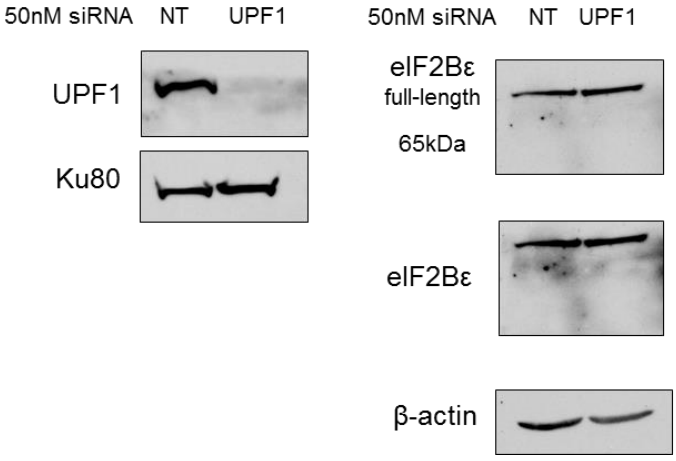

Figure 3.6: Knockdown of UPF1 to inhibit NMD does not induce expression of 65kDa eIF2Bε. Analysis of siRNA knock-down efficiency of UPF1 shown to the left. Resulting impact of eIF2Bε protein expression in normoxic SQ20B cells shown to the right.

Search for -cis and -trans regulators of alternative splicing of *EIF2B5*

To identify potential regulators mediating retention of intron 12 in *EIF2B5*, I utilized the AVISPA tool (105) to carry out a motif analysis of the locus encompassing *EIF2B5* exons 12-14. The data revealed a weak splice site at the intron12:exon13 junction, as well as a possible “GTGAG” splice site downstream of exon 13 (Fig 3.7A). Notably, these motifs were not identified in a search of additional loci within *EIF2B5*. As a control, four additional exon triplets within *EIF2B5* (exons 6-8, 7-9, 8-10, and 9-11) were used to predict the occurrence of alternative splicing using AVISPA. These loci were not predicted to be alternatively spliced. Altogether, these results suggest that alternative splicing is significantly more likely to occur at intron 12 locus compared to the upstream exon triplets tested. An additional non-motif search of regulatory sequence features in this locus identified the intron immediately downstream of intron 12 as relatively unstructured (Fig 3.7B). Furthermore, there is a short distance between exon 13 and the first AG upstream. Both features are known to contribute to weaker splicing potential (106, 107).

The motif analysis also identified potential trans regulators with binding sites within this locus which are experimentally predicted to regulate splicing of this region (Fig 3.7A). Interestingly, several of the splicing factors predicted to have the greatest impact on regulation of this locus also changed expression under hypoxia, including *SRSF2*, *SRSF3*, *HNRNPC*, *HNRNPF*, and *RBMX* (hnRNP-G) which were repressed at the mRNA level and *CELF5* which was induced (Fig 3.1A, FC ≥ |1.2|, FDR < 5%). Upon closer examination of these splicing factors, we focused in on SRSF3 and CELF5 as prime candidates to test as regulators of *EIF2B5* splicing, due to a large number of binding sites near the intron12:exon13 junction and that these factors showed >2-fold changes in mRNA expression under hypoxia.

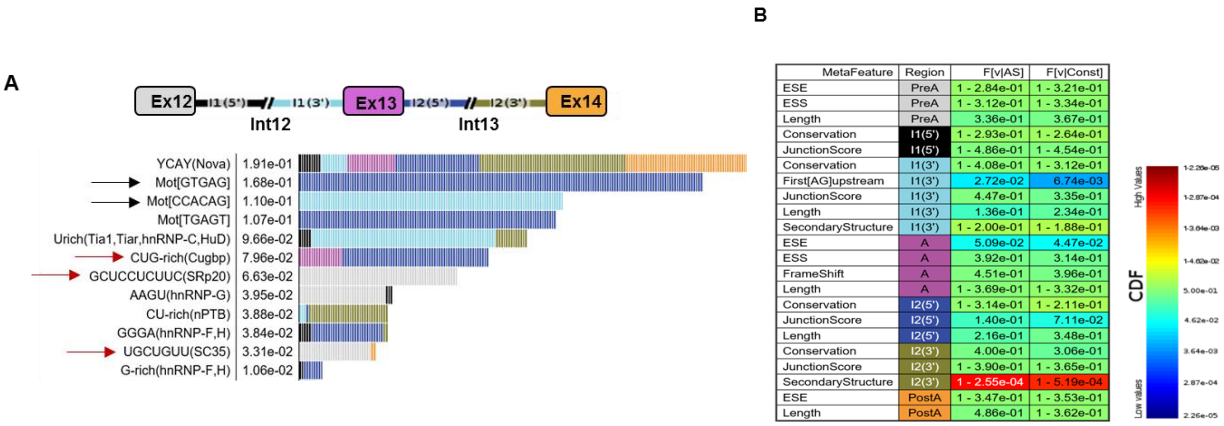

Figure 3.7: Analysis of RNA binding factor motifs and regulatory sequence features at the *EIF2B5* intron12 locus. A: Splicing factor motifs determined to have the largest effects on regulation of the *EIF2B5* exons 12 – 14 shown, with color-coded gene map above and predicted motifs shown below. Black arrows highlight a predicted weak splice site before exon 13 and an alternate "GTGAG" splice site after exon 13. Red arrows signify hypoxia-responsive splicing factors. B: Non-motif analysis of other sequences influencing splicing of *EIF2B5*. Data generated using AVISPA (47).

I next assayed for changes in protein expression of these splicing factors in hypoxic cells and observed a reproducible hypoxia-induced increase in SRSF3 protein (Fig 3.8A) and a slight decrease expression of CELF5. To test for their requirement in the splicing of *EIF2B5* and production of the resulting 65kDa protein isoform, I used siRNA to knockdown expression of these factors and assayed for changes in expression of 65kDa eIF2Bε. Upon knockdown of SRSF3, I saw a concurrent disappearance in the

expression of the 65kDa isoform of eIF2Bε in conditions of normoxia or hypoxia (Fig 3.8B,C), while siRNAs against other RBPs, such as CELF5, did not display the same effect.

RNA immunoprecipitation assays were next carried out to confirm a direct interaction between SRSF3 protein and *EIF2B5* RNA. The data showed enrichment of SRSF3 at three exons in the locus containing *EIF2B5*_intron12 (Fig 3.8D), validating the predicted binding sites observed in other systems. Furthermore, binding of SRSF3 was increased in hypoxic cells relative to normoxic cells, providing additional support for the role of SRSF3 in regulating hypoxia-induced retention of intron 12.

Figure 3.8 (Next page): Functional investigation of SRSF3 contribution to *EIF2B5* intron 12 retention. A: Immunoblot of SQ20B lysates to test expression of SRSF3 (Nx = normoxia, Hx = 16h 0.5% O_2). B: Immunoblot analysis of knock-down efficiency of SRSF3 for SQ20B cells (same experiment as panel C). C: Immunoblot of lysates collected from SQ20B cells treated with 50nM siRNA under 16h 0.5% O_2. D: Immunoblot from immunoprecipitation of SQ20B lysates with SRSF3 antibody in normoxia and hypoxia. Rabbit IgG was used as a control. RT-qPCR analysis of RNA isolated from the immunoprecipitation with SRSF3 using primers for (-) control (a region of GAPDH predicted to contain no binding of SRSF3), and primers for three exons in the region of *EIF2B5*_intron12 predicted to have SRSF3 binding.

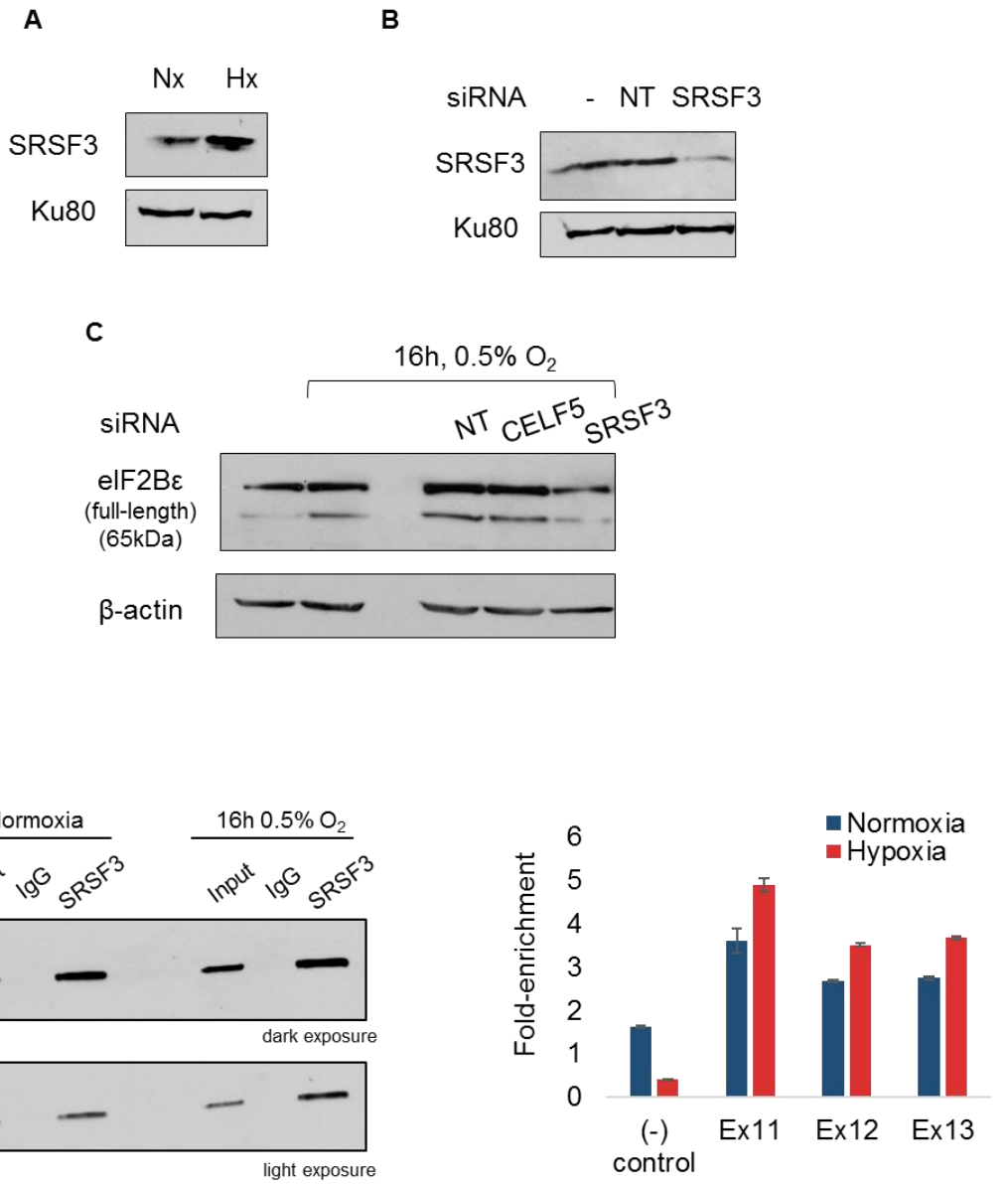
A
Nx
Hx
SRSF3
Ku80
B
siRNA
-
NT
SRSF3
SRSF3
Ku80
C
16h, 0.5% O2
siRNA
NT
CELF5
SRSF3
eIF2Bε
(full-length)
(65kDa)
β-actin
D
Normoxia
16h 0.5% O2
Input
IgG
SRSF3
Input
IgG
SRSF3
37 kDa
20 kDa
dark exposure
light exposure
Normoxia
Hypoxia
Fold-enrichment
6
5
4
3
2
1
0
(-)
control
Ex11
Ex12
Ex13

Hypoxia-mediated changes in regulation of RNA polymerase II may influence retention of *EIF2B5* intron 12

In addition to the influence of sequence elements, mRNA splicing is a co-transcriptionally regulated process which is impacted by coordination of RNAPII. Phosphorylation of the C-terminal domain (CTD) of RNAPII is known to impact the rate of transcriptional elongation, pausing, and the relative rate of splicing (108, 109). Therefore, I assayed for changes in phosphorylation of the C-terminal domain (CTD) of the largest subunit of RNAPII in HNSC cells. Surprisingly, we saw a large (>10-fold) and reproducible increase in levels of phosphorylation at serine 2 residues and a concomitant decrease in phosphorylation of serine 5 and 7 residues of the CTD in hypoxic cells compared to normoxic controls (Fig 3.9A). Interestingly, accumulation of the phospho-Ser2 form of RNAPII has been associated with retained introns compared to constitutively spliced introns (110). To assay for changes in binding of total and phospho-Ser2 RNAPII, we used chromatin-immunoprecipitation followed by qPCR. We observed a significant hypoxia-induced enrichment in both forms of RNAPII at intron 12, but did not detect the same enhanced binding at another nearby intron of *EIF2B5* which did not undergo intron retention under hypoxia (Fig 3.9B). In strong support of these data, cells expressing mutant forms of RNA polymerase with slower elongation rates led to extensive changes in mRNA splicing including specific retention of *EIF2B5*_intron12 (61). Moreover, 31 of 100 genes we identified to be affected by intron retention in hypoxia were classified as “rate-sensitive” and displayed altered expression in the RNA polymerase elongation mutants (61), suggesting that hypoxia-mediated changes in elongation of RNAPII likely influences splicing of additional loci.

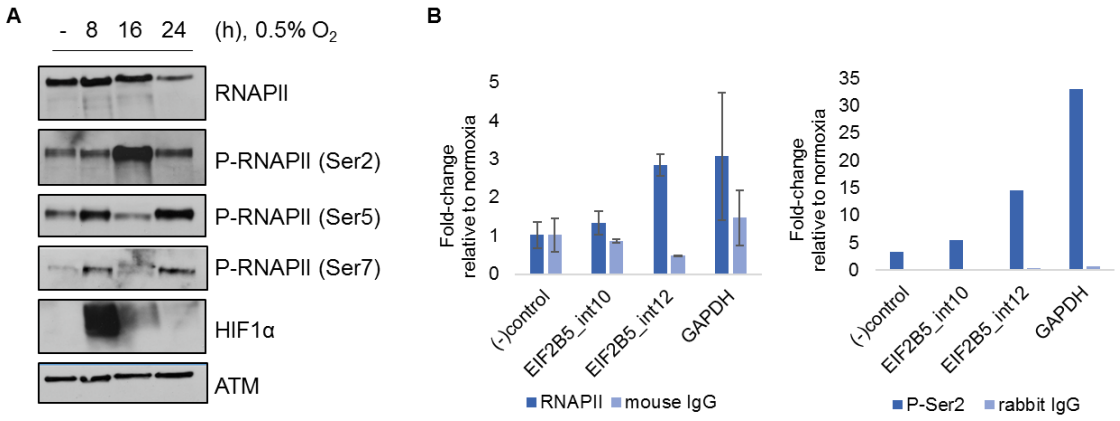

Figure 3.9: Detection of hypoxia-mediated changes in phosphorylation and binding of RNAPII. A: Immunoblot of phosphorylated forms of RNAPII in SQ20B cells. B: Chromatin immunoprecipitation followed by qPCR to determine abundance of total RNAPII or P-Ser2 RNAPII at EIF2B5 intron 12, an upstream negative control intron 10, a negative control region of GAPDH ((-) control)) and a RNAPII positive control region of GAPDH. For panel B - total RNAPII data represent average of n = 3 independently conducted experiments (error bars = S.E.M.) and P-Ser2 data shown as an average of n = 2 independently conducted experiments.

Those genes alternatively spliced in conditions of slow elongating RNAPII generally exhibited weaker 3' splice sites compared to loci insensitive to changes in elongation rate (61), so we next carried out an analysis of splice site strength for genes affected by intron retention under hypoxia. This analysis detected significantly weaker 3' splice sites for genes with changes in retained introns under hypoxia compared to a control set of splice sites not affected by hypoxia (Fig 3.10A). Collectively, differential binding of SRSF3 at the locus of *EIF2B5* intron12, a weak splice site coupled with an alternate splice site, and increased binding of total and P-Ser2 RNAPII provide strong evidence to support differential splicing of this locus and specific inclusion of intron 12 (Fig 3.10B).

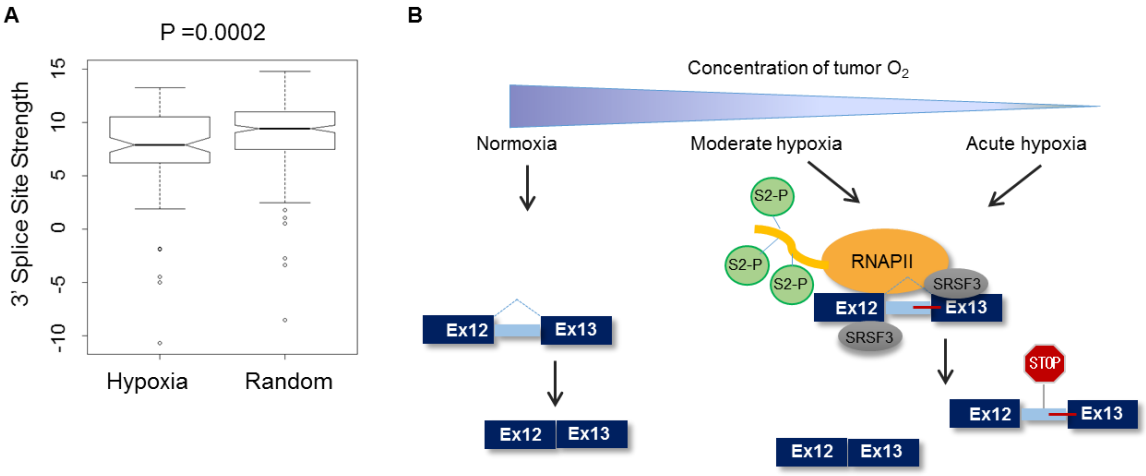

Figure 3.10: Analysis of splice site strength in hypoxia-mediated intron retention and model of *EIF2B5* intron retention under hypoxia. A: Analysis of 3' splice sites carried out using a First Model Markov method to determine maximum entropy scores, reported as 3' splice site strength (1). Hypoxia group = 101 unique 3' splice sites of introns retained under hypoxia; Random group = 252 hg19 3' splice sites. B: Under acute or prolonged hypoxia, increased phosphorylation of Ser2-RNAPII accumulates specifically at *EIF2B5* intron 12. Hypoxia increased binding of SRSF3 at this locus, where a weak splice site and alternate downstream splice site all contribute to retention of intron 12. Thus, oxygen deprivation leads to an accumulation of intron-12 containing *EIF2B5* transcripts which result in a truncated reading frame due to insertion of a termination codon.

The 65kDa isoform of eIF2Bε acts in opposition to full-length eIF2Bε to inhibit protein synthesis

Next, I tested whether the expression of 65kDa eIF2Bε has an impact on the biological function of the endogenous, full-length eIF2Bε protein. The truncated protein isoform created from retention of intron 12 is predicted to lack two critical domains which occur in the C-terminus (Fig 3.5A): a guanine nucleotide exchange (GEF) domain and a region required for interaction with eIF2α (111). Thus, I hypothesized that the 65kDa isoform of eIF2Bε would inhibit translation and lead to reduced protein synthesis. To test this, I constructed a plasmid expressing the truncated 65kDa isoform using site-directed mutagenesis to insert a stop codon within 3 nucleotides from where retention of intron 12 results in a PTC (Fig 3.11A). Expression of this mutated version of eIF2Bε under normoxic conditions resulted in the appearance of a 65kDa protein isoform consistent with the size of the endogenous protein that is induced under hypoxia (Fig 3.11B).

To analyze the impact of expression of the truncated isoform on protein synthesis, I used pulse-labeling of ^{35}S methionine/cysteine in cells expressing 65kDa eIF2Bε, full-length eIF2Bε or empty vector. There was a pronounced and reproducible decrease (approx. 30%), in total protein synthesis in cells expressing 65kDa eIF2Bε (Fig 3.11B,C) compared to empty vector, while expression of full-length eIF2Bε did not have the same effect. Translation was assessed relative to cells expressing empty vector as a control because endogenous full-length eIF2Bε remains stably expressed under hypoxic conditions and is not induced. Additionally, expression of full-length eIF2B has been shown to destabilize of ternary complex formation (112). In support of these data, I also observed a decrease in the total polysome profile of cells expressing 65kDa eIF2Bε compared to control (Fig 3.11D), and comparable to the decrease in translation observed in hypoxic conditions (Fig 3.11E).

Figure 3.11 (Next page): Expression of a 65kDa isoform of eIF2Bε leads to a global decrease in protein synthesis. A: Site-directed mutagenesis was used to introduce a stop codon into *EIF2B5* (within one codon of where intron retention introduces an early stop). B: Expression of full-length (WT) or mutated eIF2Bε (mutant) was performed for 24h in SQ20B cells (upper), followed by pulse-labeling with ^{35}S methionine/cysteine (lower) to measure changes in protein synthesis compared to expression of an empty vector pCMV6-AC (EV). Cells treated with cyclohexamide (CHX) were used as a control for inhibition of translation initiation. C: Image quantification of total ^{35}S signal from autoradiographs of 4 independently conducted experiments. Data collected from n = 4 independently conducted experiments, *P <0.01 (Student's t-test). D: Polysome profile depicts SQ20B cells expressing the 65kDa isoform of eIF2Bε for 36h compared to cells expressing control pCMV6-AC, with supporting immunoblot shown above. E: Polysome profiling of hypoxic vs. normoxic SQ20B cells.

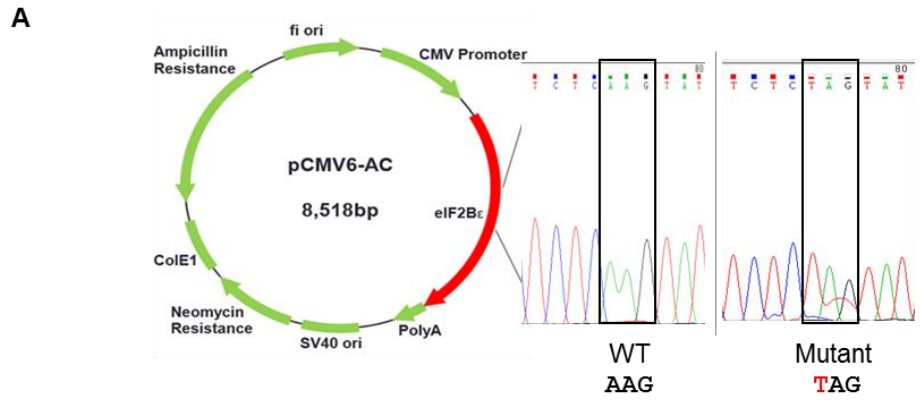
A
fi ori
Ampicillin Resistance
CMV Promoter
pCMV6-AC
8,518bp
eIF2Bε
ColE1
Neomycin Resistance
SV40 ori
PolyA
WT
AAG
Mutant
TAG

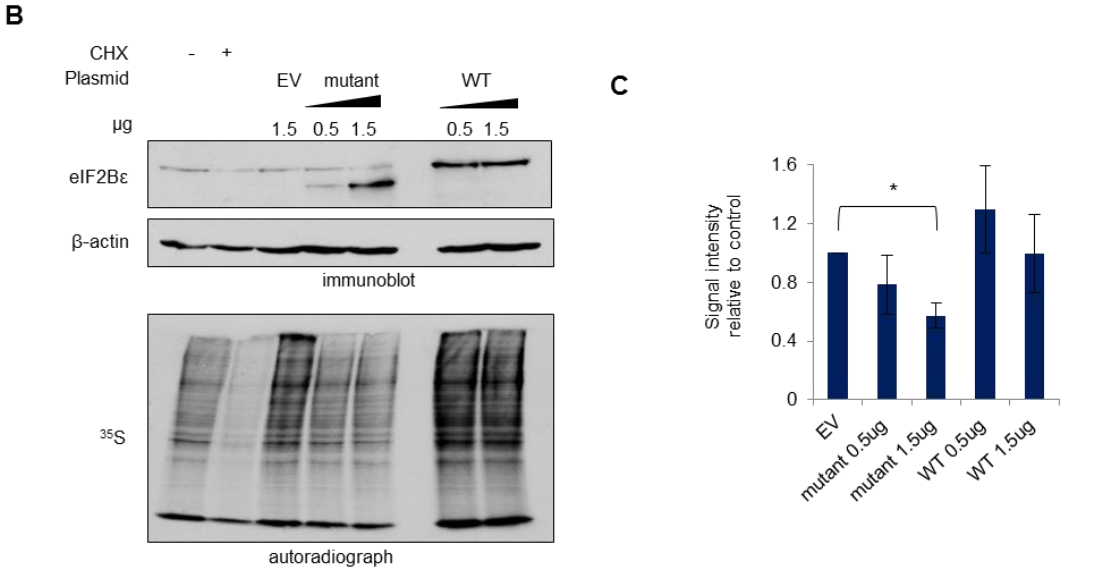
B
CHX - +
Plasmid EV mutant WT
μg 1.5 0.5 1.5 0.5 1.5
eIF2Bε
β-actin
immunoblot
35S
autoradiograph
C
Signal intensity relative to control
1.6
1.2
0.8
0.4
0
*
EV
mutant 0.5ug
mutant 1.5ug
WT 0.5ug
WT 1.5ug

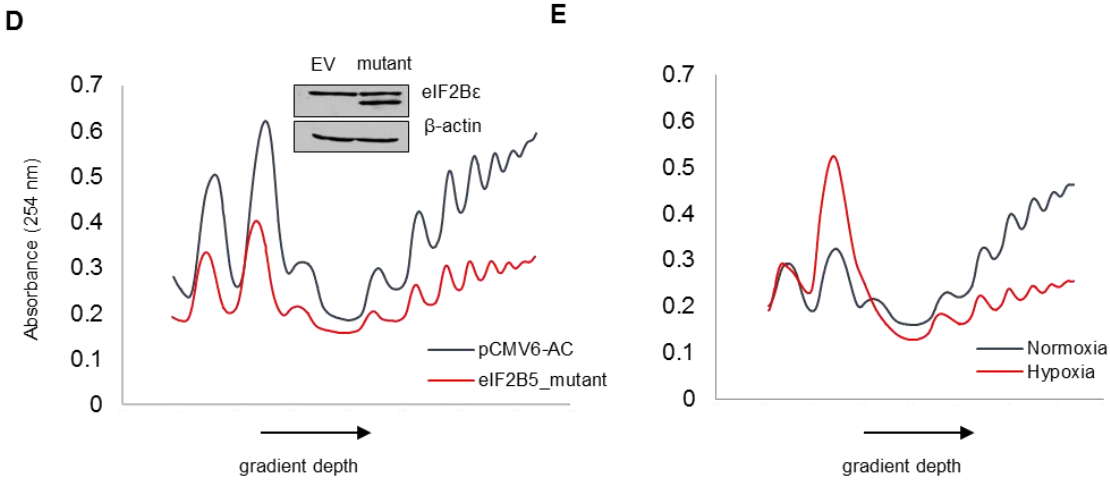
D
EV mutant
eIF2Bε
β-actin
Absorbance (254 nm)
0.7
0.6
0.5
0.4
0.3
0.2
0.1
0
pCMV6-AC
eIF2B5_mutant
gradient depth
E
0.7
0.6
0.5
0.4
0.3
0.2
0.1
0
Normoxia
Hypoxia
gradient depth

Expression of 65kDa eIF2Bε promotes cellular adaptation to hypoxia

Because downregulation of translation is one mechanism by which tumors cells overcome hypoxic stress (8), I predicted that expression of 65kDa eIF2Bε and the resulting repression of translation may promote survival of hypoxic cells. To test this, clonogenic assays were performed to measure survival and proliferation. The surviving fraction of cells expressing 65kDa eIF2Bε decreased under normoxic conditions, but was significantly higher when cells were grown in 0.5% O_2 conditions for either 16h (Fig 3.12A) or 24h (Fig 3.12B).

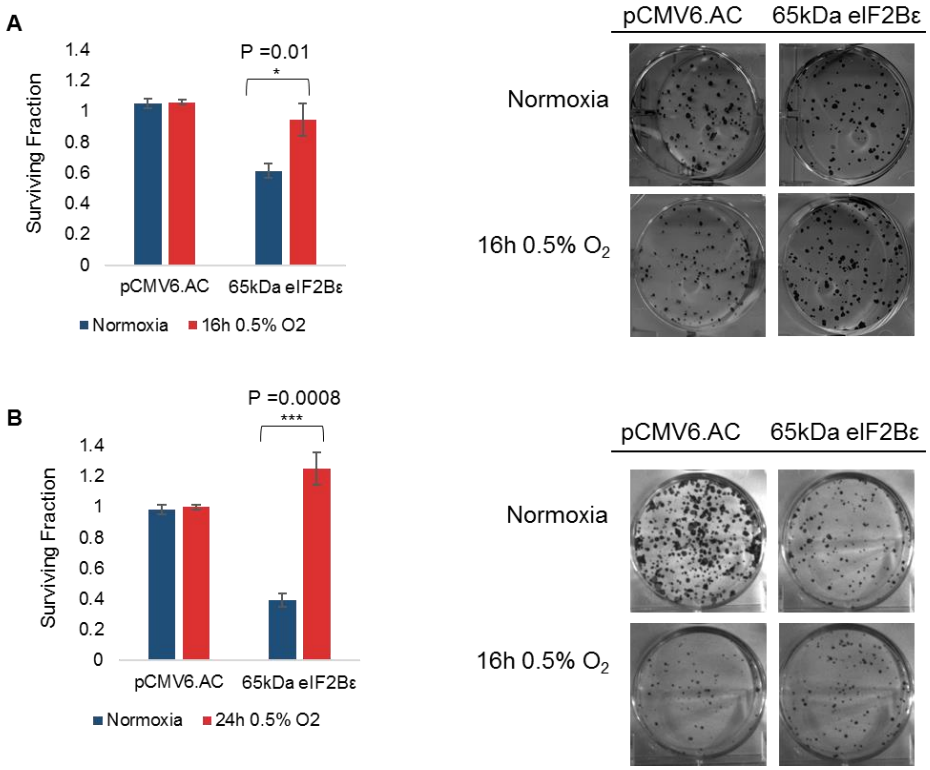

Figure 3.12: Expression of 65kDa eIF2Bε confers a survival advantage under hypoxia. A: Clonogenic assay of SQ20B cells expressing control plasmid (pCMV6.AC) or 65kDa eIF2Bε in normal oxygen or 0.5% O_2 for 16h. Analysis of three biological replicates quantified to right (P-value reported for student's t-test). B: Same experiment repeated at 0.5% O_2 for 24h. Analysis of three biological replicates quantified to right (P-value reported for student's t-test).

Discussion

I believe that these findings represent the first case of splicing as a previously uncharacterized mode of translational control under conditions of hypoxia. I demonstrate that decreased oxygen in cancer cells leads to extensive changes in mRNA splicing, resulting in a striking increase in retention of over 100 introns. A unique hypoxia-induced intron retention in the master regulator of translation initiation, *EIF2B5*, leads to a previously undescribed 65kDa isoform of eIF2Bε, that decreases overall protein synthesis in HNSC cells. Full-length eIF2Bε is a necessary component of the eIF2B complex, containing both the active GEF domain and a region for association with eIF2α (47); this complex binds eIF2α and exchanges GDP for GTP to initiate translation. During hypoxia, eIF2α is phosphorylated and translation initiation is inhibited, and was demonstrated to be critical for cell survival under extreme hypoxia. However, hypoxia-induced phosphorylation of eIF2α is reversible and not long-lasting (8). Thus, I propose that during periods of acute or prolonged hypoxia, intron retention in *EIF2B5* leads to expression of a truncated dominant-negative isoform to further inhibit protein synthesis in cancer cells (Fig 3.13). Expression levels of 65kDa eIF2Bε are consistently upregulated in hypoxia, with the greatest induction of this isoform observed at stringent (0.2% O_2) and prolonged (≥16 h) hypoxic conditions. Altogether, these data establish a biological role for the 65kDa isoform of eIF2Bε in promoting adaptation to hypoxic stress in cancer cells. The question remains as to whether induction of this isoform is a cause or effect of tumorigenesis. The results from the clonogenic assay suggest a role for 65kDa eIF2Bε in tumor growth, however additional animal studies to evaluate its potential to influence tumor formation are needed and will be a focus of future work.

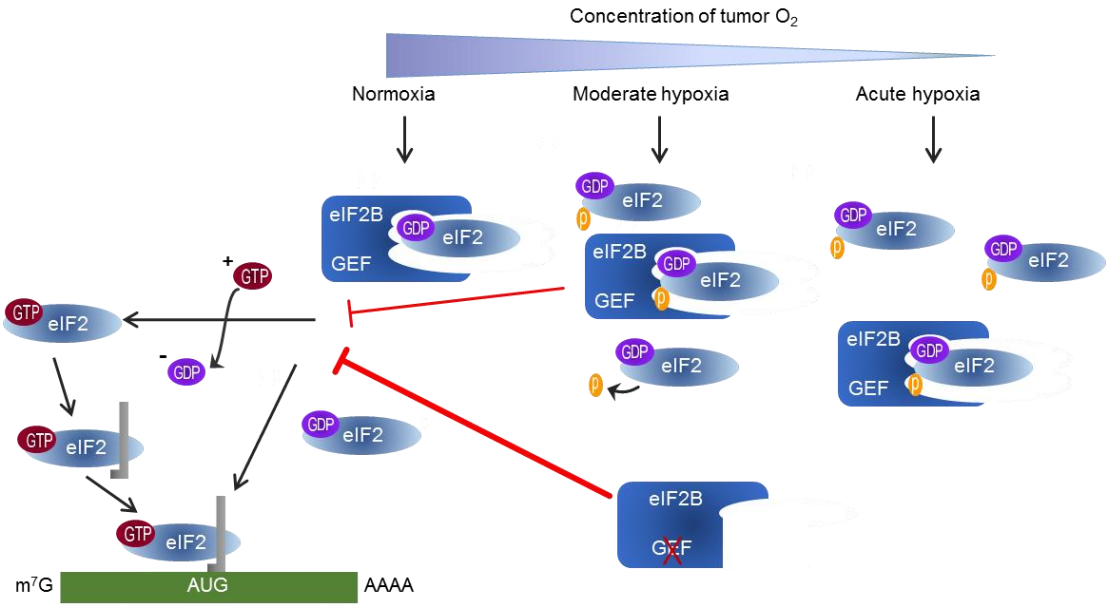

Figure 3.13: Model of the role of the hypoxia-induced 65kDa isoform of eIF2Bε in inhibiting translation initiation during periods of prolonged or acute hypoxia. Retention of intron 12 under hypoxia leads results in a 65kDa isoform of eIF2Bε. This isoform lacks the functional guanine exchange factor (GEF) domain and acts opposite to the full-length isoform to inhibit translation during periods of prolonged hypoxia.

Regulation of intron 12 retention in *EIF2B5*, like splicing of most loci, appears to be influenced by several factors, including a weak splice site, secondary structure of *EIF2B5* transcripts, and binding and coordination of RNA processing factors and spliceosome machinery. Unique sequence features may also explain why some introns are retained under stress while others are not. Retained introns are short and high in GC content (113, 114). Intron 12 is relatively shorter and higher in GC content, compared to other introns in *EIF2B5*, suggesting that sequence elements in this region may specifically promote retention of intron 12 compared to other introns. In addition, the AVISPA analysis of sequence features detected a relatively weaker splice site at exon 13 and a possible “GT” alternate splice site in intron 13, which likely influence splice site

choice at the junctions surrounding intron 12 under hypoxic stress. Additionally, I observed downregulation of many genes that regulate splicing and RNA processing, including some of which were predicted to bind at the *EIF2B5*_int12 locus. There is evidence that global downregulation of splicing factors and RNA binding proteins can promote intron retention in a regulated manner during other physiological responses or processes, such as hematopoiesis (3). However, I uncovered that the splicing factor predicted to contain the most binding sites within the *EIF2B5*_intron12 locus, SRSF3, was induced at the protein level under hypoxia and exhibited increased binding at *EIF2B5* exons 12 and 13 under hypoxia (Fig 3.8). Reducing levels of SRSF3 decreased expression of the 65kDa protein isoform, suggesting a major role of SRSF3 in regulating splicing and intron retention in *EIF2B5* in hypoxic cells.

Regulation of *EIF2B5* intron 12 as well as additional introns retained under hypoxia are likely influenced by hypoxia-mediated changes in activity of RNAPII. Under hypoxia, changes in phosphorylation of the C-terminal domain of RNAPII influence expression of HIF-1α target genes by affecting the binding of co-factors and the kinetics of transcriptional activation (92). Hypoxia-mediated changes in the rate of transcriptional elongation may explain why we observed an enrichment of splicing changes at the 3' end of genes (i.e. ALE, TUTR and RI categories). Several RNA binding proteins, including polyadenylation factors and splicing regulators interact specifically with phospho-Ser2 modifications of the CTD (115). Intriguingly increased occupancy of phospho- Ser2 RNAPII is associated with retained introns compared with constitutively spliced introns (110). Our data support that this mechanism may act to promote retention of intron 12 in *EIF2B5*, and future work by our group will determine whether this translates to other hypoxia-induced retained introns as well. This regulation could depend on differences in -cis sequences around the splices site, which have been

reported to occur in genes sensitive to changes in RNAPII elongation events(61); likewise, our data showed an enrichment for relatively weak 3' splice sites at genes affected by intron retention under hypoxia compared to control genes (Fig 3.10A).

The physiological relevance of these findings is underscored by the fact that *EIF2B5* intron 12 is expressed in multiple types of cancer known to contain hypoxic fractions and more importantly, is overexpressed in tumor vs. normal tissues of HNSC patients. Intron retention has now been observed in most cancers, further highlighting the need to understand this important form of RNA processing and regulation in a cancer context. My data suggest that many hypoxia-responsive isoforms have the potential to influence key biological pathways in cancer cells. For example, the retained intron in *TGFB1* leads to a different 5' UTR and alternate transcription start site, which would code for a 416 amino acid peptide instead of the full-length 689 amino acids. This change in the C-terminus would affect part of a FAS1 domain, involved in binding integrin to regulate cell adhesion, as well as an EMI domain which is thought to be a protein-protein interaction domain. These data highlight the need to include alternative splicing and individual mRNA transcript levels in gene expression studies to investigate cellular adaptation to hypoxia, as well as include these changes in splicing in the development of prognostic hypoxia gene expression signatures.

CHAPTER 4

Discussion & Future Directions

Summary

Here I presented evidence that under acute or prolonged hypoxia, alternative splicing leads to a retained intron in the master regulator of translation initiation, *EIF2B5*. Strikingly, retention of this intron creates a phylogenetically conserved pre-termination codon which results in a truncated form of eIF2Bε lacking the enzymatic GEF activity. A resulting truncated isoform of eIF2Bε is induced under hypoxia, which acts in opposition to full length eIF2Bε to inhibit protein translation and confer a survival advantage to hypoxic cells.

EIF2B5 was among 100 genes with changes in intron retention in conditions of low oxygen. Surprisingly, over 95% of these genes showed an increase in a retained intron under hypoxia, providing evidence that regulated control of intron retention is a way to exert fine control over the repertoire of hypoxia-responsive mRNA isoforms expressed in cancer cells. In support of this notion, these genes were functionally enriched to carry out biological roles critical to cellular adaptation to hypoxia, such regulation of cell cycle, gene expression, RNA splicing and programmed cell death (Fig 3.1, DAVID Gene Ontology, $P< 0.05$). This class of genes may be commonly regulated by a combination of relatively weak 3' splice sites (Fig 3.9, 3.10) and accumulation of a form of RNA polymerase II (RNAPII) phosphorylated on serine 2 residues of the C-terminal domain. These data open up a novel area of investigation to study the contribution of hypoxia-mediated phosphorylation of RNAPII in regulation of intron retention in hypoxic cells.

Control of intron retention in hypoxic cells: investigating the impact of changes to RNAPII elongation & co-transcriptional processing

Regulated pausing of RNAPII near promoters is one mechanism to control expression of stress responsive genes, including genes that respond to oxygen deprivation. The C-terminal domain (CTD) tail of the largest subunit of RNAPII, Rpb1, contains 52 repeats of the peptide sequence, “YSPTSPS.” Phosphorylation of serines 2, 5 and 7 play roles in regulating several steps of transcription including initiation, elongation and termination (116). Under moderate hypoxia, the hypoxia-inducible transcription factor, HIF-1α, enhances recruitment of two complexes (Mediator/CDK8 and the Super Elongation Complex) at target gene promoters, which in turn impact phosphorylation of the CTD of RNAPII to control transcriptional elongation (92). While phosphorylation of RNAPII-Ser2 along with phospho-Ser5 regulate release and productive elongation of RNAPII to initiate transcription, P-Ser2 is also observed in increasing amounts moving toward the 3’ end of genes. In the context of splicing, phosphorylation of the CTD has impacts on mRNA processing beyond transcriptional activation, with as many as 100 proteins observed to associate with the CTD (117). Several RNA binding proteins with roles in 3’ end processing of nascent transcripts, including polyadenylation factors such as PCF11 and splicing regulators CDK12 and CDK13, interact specifically with phospho-Ser2 of the CTD (115). Additionally, binding of P-Ser2 RNAPII is significantly enriched at retained introns compared to constitutively spliced introns (110). Although hypoxia-mediated changes in phosphorylation of the CTD have not yet been linked to regulation of splicing, I demonstrated increased binding of total and phospho-Ser2 forms of RNAPII at the retained intron 12 of *EIF2B5* under hypoxia (Fig 3.1), providing support that increased

phopsho-Ser2 may contribute to changes in splicing of hypoxic cells, specifically by promoting retention of select introns.

The RNA-Seq data revealed differential expression of genes regulating RNAPII in hypoxic cells (Fig 2.1) and a large and reproducible increase in levels of phosphorylation at serine 2 residues at several different durations of low oxygen (Fig 3.14). In the context of regulated intron retention, several groups have specifically linked slowly elongating or paused RNAPII to changes in splicing, including increased intron retention (2, 61, 115, 118). This regulation is influenced by stressors such as UV exposure, -cis RNA sequences and co-factors which interact with the CTD of RNAPII. Unsurprisingly, I observed that each of these factors contributed to increased retention of intron 12 in *EIF2B5* (see Figs 3.2-3.5, 3.9). While these data provided strong preliminary evidence to implicate changes in transcription rate and regulated intron retention in conditions of hypoxia, additional experiments aimed to examine the causal link between hypoxia-induced changes in phosphorylation of RNAPII and increased intron retention are needed.

To start, cells should be collected for immunoblot analyses at additional concentrations of oxygen at varying time-points to better understand the dynamics of phosphorylation at the CTD under hypoxia. Additionally, it is critical to investigate to what extent phospho-Ser2 contributes to intron retention under hypoxia by identifying how many genes with retained introns exhibit increased binding of P-Ser2 RNAPII under hypoxia. This can be addressed experimentally by either utilizing chromatin immunoprecipitation (ChIP) followed by sequencing to carry out a genome-wide scan of P-Ser2 RNAPII abundance or by targeting select introns of the 100 genes affected by

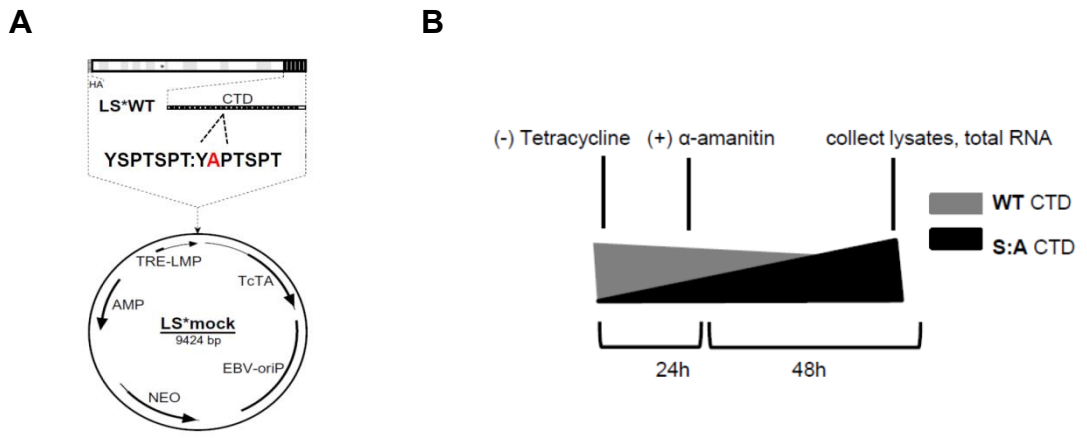

Figure 4.1: Schematic of experimental design to genetically block phosphorylation of P-Ser2 in the CTD of RNAPII. A: Tetracycline-off expression system to express the largest subunit of RNA Pol II (Rpb1) which contains the CTD repeat region in which the second serines (Ser2) have been mutated to unphosphorylatable alanines. The plasmid Rpb1 also contains a point mutation which confers resistance to the RNA Pol II inhibitor α-amanitin. (Image modified from manuscript describing initial plasmid development (2)). B: Upon removing tetracycline, expression of this S:A mutant is induced and addition of α-amanitin can be used to repress expression of endogenous Rpb1.

intron retention under hypoxia and assaying for binding of P-Ser2 RNAPII individually by ChIP-qPCR.

Furthermore, I have obtained a plasmid which expresses a form of the largest subunit of RNA Pol II, RPB1, in which the second serine of each C-terminal domain repeat series has been mutated to an alanine (115). Overexpression of this plasmid, while depleting levels of endogenous wild-type RPB1 with the drug α-amanitin (Fig 4.1), can be used to block the phospho-Ser2 form of RNAPII. These cells can then be used to test if intron retention in *EIF2B5* is reduced under hypoxia in the absence of phospho-Ser2 compared to cells with normal levels of wild-type RPB1. These studies can be extended to include the other 100 genes observed to undergo intron retention in hypoxic conditions or loci determined to show increased binding of P-Ser2 RNAPII as identified by ChIP-seq. One study identified that moderate hypoxia (1% oxygen for 24h) can

induce phosphorylation of serines 2 and 5 in HCT116 human colorectal carcinoma cells (92). These data led to a model by which regulated pauses of RNAPII at gene promoters help to coordinate the gene expression response to hypoxia. It would be fascinating to explore pausing of RNAPII beyond gene promoters and investigate how changes to the elongation rate of RNAPII are affected in hypoxic cells. In the broader context of regulated intron retention, hypoxic stress may represent an ideal model for a physiologic stress under which to investigate mechanisms that control intron retention. However, if RNAPII is a major contributor to this process, understanding exactly how hypoxia alters rates of transcription would be a critical first step. In the context of UV stress, which also induced intron retention in *EIF2B5* (as evidenced by induction of the 65kDa protein isoform), blocks to transcription elongation arise due to DNA damage caused by the UV exposure which leads to pyrimidine dimers which alter RNAPII transcription kinetics and subsequently impact regulation of splicing (118). Based on my data, hypoxia-mediated changes to changes in transcription elongation are more likely explained by changes in cell signaling and phosphorylation of the CTD. To study changes of transcription elongation more directly, global run-on (GRO) sequencing experiments could be performed in hypoxic and normoxic cells to examine how oxygen deprivation influences nascent RNAs, elongation rates and RNAPII pausing.

To characterize the -cis sequence elements with the greatest influence on intron retention, a more comprehensive analysis of RNA sequences surrounding the retained introns for all genes affected by changes in intron retention under hypoxia should be conducted. These data would allow for the characterization of common sequence features that influence intron retention under stress. Analyses to consider should include a complete evaluation of splice site strength at the 5’ and 3’ splice sites of these genes

compared to splice sites of genes unaffected by alternative splicing, a computational search for cryptic alternative splice sites at loci containing introns retained under hypoxia, an assessment of RNA secondary structure at these loci and an analysis of the lengths and GC content of hypoxia-retained introns compared to constitutively spliced introns.

Testing the functional requirement of a weak splice site and usage of an alternate downstream splice site in leading to the expression of 65kDa eIF2Bε under hypoxia could be carried out by blocking retention of intron 12 in *EIF2B5* by targeted disruption of the 3' splice sites. Then, the ability of these cells to suppress translation under hypoxia can be evaluated. These experiments would significantly add to the impact of this study, since all the work to determine the role of 65kDa eIF2Bε thus far has been carried out in the context of inducing 65kDa eIF2Bε expression, but not yet in the absence of this isoform. To solidify its requirement in the decreased protein synthesis observed in hypoxic cells, the complementary experiment would be to block the retention of intron 12 in hypoxic cells and test if translation is suppressed to a lesser degree than cells able to induce 65kDa eIF2Bε. However, to achieve this is technically difficult. Permanent genome-editing techniques, such as CRISPR, which could be aimed at removing intron 12 from the genomic locus encoding *EIF2B5,* would also impact the maturation of mRNAs expressing 80kDa full-length isoform of eIF2Bε. Even a more targeted approach to disrupt the premature-stop codon introduced by intron 12 would likely alter normal splicing of full-length *EIF2B5* transcripts since the stop codon occurs in a highly-conserved area of the 3' splice site. A way to transiently block the inclusion of intron 12 and disrupt its splicing could be to introduce anti-sense morpholinos, which will bind to complementary sequences and sterically hinder binding of splicing factors at a particular

site. Morpholinos are commonly used to disrupt alternative splicing of skipped exons, however little has been done to test their use in blocking or promoting retention of introns. Our data identified a potential mechanism for intron 12 retention by which under hypoxic stress, a weak 3' splice site at the intron12:exon13 is not used, but an alternate downstream 3' splice site may be used instead (Fig 3.7). Targeting the 3' splice site used in the normal splicing of full-length *EIF2B5* transcripts could be tested first. Morpholinos could be designed to block this 3' splice site in cells under normoxic conditions, to see if disrupting this site would promote usage of the alternate downstream 3' splice site and cause induction of the 65kDa protein isoform. Then, in a separate experiment, morpholinos designed to block binding at the alternate downstream 3' splice site could be used in hypoxic cells to validate selection of the alternate 3' splice site is necessary for expression of intron 12-containing transcripts and induction of the 65kDa protein isoform. These cells could then be used to verify that expression 65kDa eIF2Bε is required to repress translation to the fullest extent under conditions of prolonged or acute hypoxia. These studies could provide one of the first examples of targeting weak 3' splice sites to study mechanisms of intron retention under cellular stress.

Conservation of eIF2Bε: determining the action of the 65kDa isoform of eIF2Bε in regulating translation initiation

The *EIF2B5* gene is highly conserved, especially in the region containing intron 12 (Fig 3.2). Beyond the scope of hypoxic cancer cells, the action of 65kDa eIF2Bε is likely relevant to other physiologic conditions of low oxygen, such as during normal tissue

development or in non-cancerous diseases like cardiomyopathy. The eukaryotic initiation factor eIF2Bε, is a necessary component of the five member eIF2B complex. The eIF2Bε subunit contains both a region which interacts with eIF2α and a catalytic guanine nucleotide exchange factor (GEF) domain (111). Under normal conditions, eIF2B binds eIF2α and exchanges GDP for GTP to initiate translation. During hypoxia, eIF2α is phosphorylated and this process is inhibited. The data presented in Chapter 3 demonstrate that hypoxia induces intron retention in *EIF2B5* transcripts, resulting in a dominant-negative 65kDa isoform of eIF2Bε which may act in parallel to phospho-eIF2α to further reduce translation in periods of acute or prolonged hypoxia. The hypoxia-induced isoform of eIF2Bε is predicted to lack a portion of the C-terminus containing the catalytic (GEF) domain and a region known to interact with eIF2α (Fig 3.5). Additional work to identify the general mechanistic action of this isoform on translation initiation in both normal and cancer cells could support the notion that this isoform may carry out an evolutionarily conserved role in conditions of physiologic hypoxia in normal tissues.

To begin, experiments to verify that 65kDa eIF2Bε forms inactive eIF2B complexes lacking functional GEF activity could be carried out using a plasmid harboring an N-terminal tagged version of eIF2Bε. Immunoprecipitation could be performed with cells expressing this plasmid and an antibody against the N-terminal tag. Then an immunoblot incubated with antibodies against the other eIF2B complex members could be used to test for their association with 65kDa eIF2Bε. In addition to the other complex members, antibody against total and phospho-eIF2α could also be utilized on the immunoblot to determine whether complexes containing 65kDa eIF2Bε lose some ability to interact with eIF2α. Following the experiments to study the formation of the eIF2B complex, assaying for the GEF activity of complexes containing either full-length or

65kDa eIF2Bε would provide direct evidence for the 65kDa isoform acting as a dominant-negative to oppose the function of full-length eIF2Bε.

Additional studies to further delineate the relationship between inhibition of translation due to phospho-eIF2α or caused by induction of 65kDa eIF2Bε would also strengthen the hypothesis of a conserved role for 65kDa eIF2Bε. Adaptation of cells to hypoxia entails adjusting key metabolic processes to reduced energy availability emanating from lower oxygen availability (9, 32, 119). Control of translation initiation has been specifically shown to contribute to downregulation of protein synthesis under hypoxia, which occurs through phosphorylation of eIF2α by hypoxia-mediated induction of the integrated stress response (ISR) (97). An interesting observation from my work showed that upon siRNA knockdown of eIF2Bε, there was delayed induction of phospho-eIF2α (Fig 3.5). I believe this further supports the notion that induction of 65kDa eIF2Bε acts in parallel with stress-induced phosphorylation of eIF2α to maintain suppressed translation in hypoxic conditions. Perhaps when levels of 65kDa eIF2Bε become too high, cells can no longer tolerate immediate and long-lasting phosphorylation of eIF2α. Moreover, it has been shown that a S51A mutation blocks hypoxia-mediated inhibition of translation up to 10h under hypoxic conditions (8), but not completely. This supports the existence of a secondary mechanism to inhibit protein synthesis in conditions of hypoxia. To investigate the cross-talk between these two pathways, expression of 65kDa eIF2Bε should be induced in cells expressing non-phosphorylatable eIF2α. This could be achieved by either using cells with the S51A serine:alanine mutation to block phosphorylation of eIF2α or by adding expression of GADD34 (the phosphatase able to remove phosphoryl groups from eIF2α (48)) in these cells. While we observed that thapsigargin-induced ER stress did not lead to an

induction of 65kDa eIF2Bε, it would be interesting to test if other ISR initiators, such as nutrient deprivation, upregulate 65kDa eIF2Bε to see if these two pathways converge during other cellular stress responses.

Investigating the tumorigenic potential of 65kDa eIF2Bε

The clinical relevance of these findings is emphasized by the fact that *EIF2B5* intron 12 is expressed in several types of solid cancer known to contain hypoxic fractions and is overexpressed in tumor versus normal tissues of head and neck cancer patients (Fig 3.4). While mutations in *EIF2B5* have been linked to Vanishing White Matter Disease (120), there have not yet been reports of mutations in *EIF2B5* in association with cancer. However, defects in eIF2B guanine nucleotide exchange activity have been observed in a model of oncolytic virus infection in mouse embryonic fibroblasts (121). The authors posit that this alteration in the GEF function is due to upregulation of full-length eIF2Bε in transformed versus primary mouse embryonic fibroblasts. However, it would be interesting to look for activation of the 65kDa isoform of eIF2Bε in this model and to test cellular sensitivity to the oncolytic vesicular stomatitis virus in the presence and absence of 65kDa eIF2Bε. From what I have gleaned about the function of 65kDa eIF2Bε in downregulation translation in our system, I predict that blocking induction of this isoform may promote susceptibility to oncolytic viruses and subsequently prevent tumorigenesis in these cells.

An essential question about the role of 65kDa eIF2Bε in tumor growth is whether induction of this isoform is a cause or effect of tumorigenesis. The results from the clonogenic assay suggest a role for 65kDa eIF2Bε in tumor growth (Fig 3.12). Moreover,

immunoblot analyses of tumors established with SQ20B cells in mice showed elevated levels of 65kDa eIF2Bε in tumor relative to normal tissue (Fig 4.2) supporting this idea. However, additional cancer cell assays and animal studies are necessary to fully evaluate its potential to influence tumor formation. Experiments to test the influence of 65kDa eIF2Bε on tumor growth and formation should first be carried out *in vitro* for several cancer cell lines and include testing for induction of 65kDa eIF2Bε in higher and lower concentrations of oxygen to mimic the range of oxygen levels observed in malignant tissues, performing soft agar assays to test for anchorage-independent cell growth and developing cell lines stably expressing 65kDa eIF2Bε for future animal work.

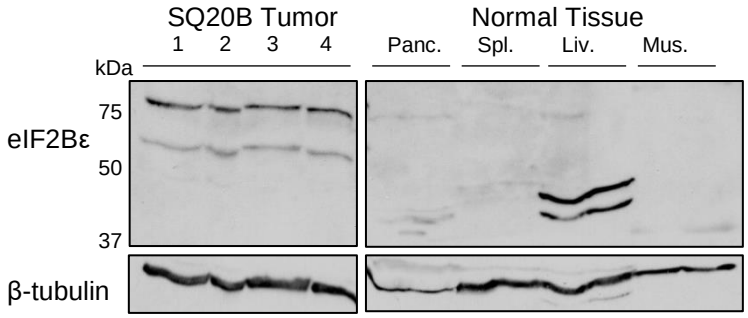

Figure 4.2: Expression of 65kDa eIF2Bε is observed in tumors established with SQ20B cells in nude mice. Left shows lysates prepared from four different tumor samples harvested from four different mice. Normal tissue samples are included to the right. All samples were processed on the same immunoblot for direct comparison. (Tissue abbreviations: Pancreas, Spleen, Liver, Muscle).

Lysates prepared from tumor and control tissues from tumor-bearing mice of varying ages can be used to determine how early during tumor formation the endogenously expressed 65kDa eIF2Bε isoform is induced. To assay for the tumorigenic potential of 65kDa eIF2Bε, tumors can be established in mice using cells stably expressing 65kDa eIF2Bε to test if this isoform influences the time for these mice to develop tumors, the size of tumors and overall survival. Since the clonogenic assays identified a survival advantage in cells expressing this isoform under hypoxia, it would also be interesting to test if mice with tumors expressing high levels of 65kDa eIF2Bε contain more hypoxic areas that are surviving and become more resistant to radiation or chemotherapies compared to mice with endogenous expression of eIF2Bε.

Implications for refining prognostic gene expression signatures in solid cancers

Altered regulation of splicing represents a naturally occurring mechanism by which stress-responsive or tumor-specific isoforms that may contribute to tumor growth and survival can be induced. Intriguingly, intron retention has been observed to occur at higher levels in tumor tissues relative to normal tissues for most solid cancers in support of this notion (66). Preliminary analyses suggest that *EIF2B5* intron 12 is anti-correlated with survival in patients with head and neck squamous cell carcinoma (HNSC) (Fig 4.3), where I observed a modest yet significant negative correlation between the expression of the locus spanning intron 12 and exon 13 and overall survival (R= -0.101, P = 0.017, Fig 4.2).

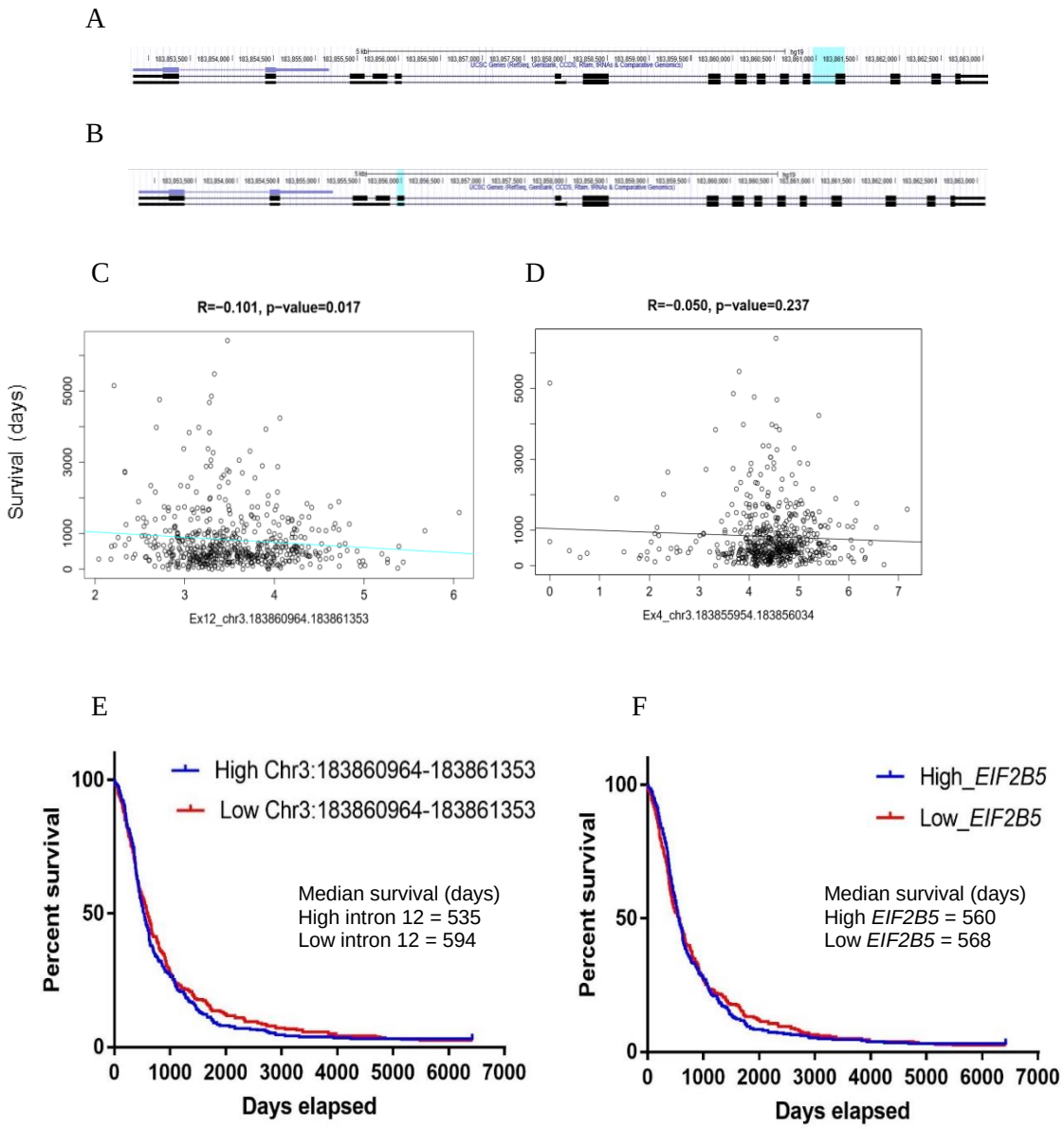

Figure 4.3: Correlation of expression of *EIF2B5* intron 12 with patient survival in HNC. A,B: Gene maps of *EIF2B5* on chromosome 3 displaying the exon probes used for expression/survival correlation analysis highlighted in light blue (modified from the UCSC Genome Browser). A= intron 12 locus; B= control locus. C,D: Expression (RPKM) of the locus encompassing intron 12 through exon 13 (chr3: 183860964-183861353) is correlated with overall survival for 549 HNSC patients, while expression of exon 4 is not. E, F: Kaplan Meier survival analysis conducted for the locus containing intron 12 compared to expression of the total *EIF2B5*.

However, expression of other exons in *EIF2B5* which were unaffected by alternative splicing did not significantly correlate with survival (Fig 4.2). Kaplan Meier survival analysis determined that HNSC patients with high expression of the intron 12 locus had a 59-day reduction in overall median survival time compared to patients with low expression of intron 12 (Fig 4.2). While this trend did not reach statistical significance, differences in total gene levels of *EIF2B5* alone cannot explain this change in survival time, as median survival between patients with high versus low expression differed only by 8 days (Fig 4.2).

Intron retention as well as other modes of alternative splicing are emerging as key regulatory mechanisms in physiological processes such as hematopoiesis and pathological conditions such as malignancy. Understanding the regulation and biological role of hypoxia-mediated alternatively spliced isoforms is leading to a deeper understanding of cellular adaptation to hypoxia, and this expanse in knowledge is creating new areas of investigation for targeted therapies. The work in this project has newly identified splicing as a mechanism of translational control and adaptation to hypoxia in cancer cells. Both translation and mRNA splicing pathways can be targeted in cancer, however many hurdles exist to therapeutically ablating such key biological processes. Disrupting expression of tumor-specific isoforms with key biological roles in the cellular adaptation to stresses within the tumor microenvironment may present a new avenue for targeted therapies. As such, it is critical to redevelop current prognostic hypoxia gene expression signatures to include isoform-level changes in expression.

CHAPTER 5

Materials & Methods

UV-LCM of EF-5 labeled tumors

Specifically, 9L gliosarcoma cells were used to establish tumors in a rodent model. At the experimental endpoint, animals were anesthetized and the bioreductive dye, EF5, was injected through tail vain at the concentration 30–80 mg/kg 1–2 h before tumor excision [23]. Tumors were embedded into either low melting agarose or OCT and stored at −80 °C. In order to maintain the integrity of the RNA, the tissue samples must be kept free of RNAses and DNAses, which degrade the nucleic acids. Activity of these enzymes can be partially inhibited by taking several additional measures during the preparation of tissue slides, including limiting humidity and by preparing samples at a low temperature. One tumor sample will be sectioned onto several membrane slides at a thickness of 10 μm tissue slices using a cryostat at −20 °C. Slides are processed in the same orientation to enable collection of several dissections per slide and eventual pooling of material collected from slides derived from the same tumor sample. To ensure optimal conditions, after tissues have been sectioned onto membrane slides and during the antibody staining protocol, slides are washed thoroughly and then dehydrated with ethanol. In addition, during incubation periods, slides are stored in 50-ml conical tubes containing desiccant pellets and kept on ice or in a 4 °C cold room throughout the experiment. Once slides have been stained with a secondary antibody containing fluorochrome, laser capture microdissection can be performed. Microdissection is carried out on areas of the tumor with the strongest EF5 (or other appropriate marker of hypoxia) signal to collect hypoxic samples. To avoid necrotic tissue, which will also exhibit a strong EF5 signal due to lack of oxygen, slides must also be stained with a nuclear stain, such as Hoescht, to enable researchers to distinguish hypoxic cells (with intact nuclei) from anoxic/necrotic cells (with fragmented nuclei). Areas of the same

tumor that display little to no signal from the secondary antibody are collected as paired normoxic controls (see Fig. 4.1a–c for overview; [23]). All material collected by LCM is immediately frozen on dry-ice pellets and stored at −80 °C until RNA extraction.

Cell lines & culture conditions

SQ20B cells, derived from human head and neck squamous cell cancer, were obtained from American Type Culture Collection (Rockville, MD). The RKO cells were a generous gift from Dr. Cho (University of Chicago). Both cell lines were maintained in Dulbecco's Modified Eagle Medium (DMEM) media supplemented with 4.5g/L D-Glucose, 1X L-glutamine, 10% Fetal Bovine Serum and 1X Penicillin/Streptomycin and cultured in an 37°C humidified 5% CO2 atmosphere. For oxygen deprivation experiments, cells were incubated in 37°C humidified 5% CO2 conditions with varying concentrations of O2 in an INVIVO2 400 chamber (Baker BioScience Solutions).

RNA purification

RNA was isolated from cells using the Trizol reagent (ThermoFisher), and purified according to the manufacturer's protocol. All purified RNA was subsequently treated with DNaseI digestion to remove possible DNA contaminants (Qiagen). The quality of RNA used for cDNA library preparation was verified using the RNA nano 6000 analysis chip on a BioAnalyzer 2000 series instrument (Agilent Technologies) to ensure an RNA integrity value greater than or equal to 9.

cDNA library preparation and high-throughput sequencing

The cDNA libraries for sequencing were prepared from poly(A)+-selected mRNA, according to Illumina's TruSeq Stranded mRNA sequencing preparation kit. Briefly, 1µg

RNA was purified for mRNA. Then mRNA material was fragmented and denatured, in preparation for first and second strand cDNA synthesis steps. Finally, the 3' ends were adenylated to ligate strand-specific adapter sequences to cDNA material and amplified using PCR. Purity and size of cDNA library products were confirmed using a BioAnalyzer instrument. Library concentrations were determined via RT-qPCR using the Library Quantification Kit (KapaBiosystems). The samples were then prepared and sequenced on an Illumina HiSeq Series instrument.

Analysis of RNA-sequencing data

The sequencing data were aligned using an RefSeq hg19 reference with STAR software (version 2.3.0.1)(72), resulting in an average of 1.7×10^8 uniquely aligned reads per sample. The Cufflinks software suite (version 2.1.1) was used for differential expression analysis, with standard parameters and RefSeq hg19 reference annotations. Gene ontology analyses were carried out using DAVID software (81).

The mixture of isoforms software, MISO, version 0.5.1 (February 23, 2014 release) was used for the exon-centric isoform quantification analysis (85). Each of the 4 hypoxia and normoxia replicates were merged into one, file for each treatment for MISO analysis. For the exon-centric analysis, the hg19 GFF3 annotation files for each of the splicing event categories A3SS, A5SS, AFE, ALE, MXE, RI, SE and Tandem UTR, were (downloaded from http://genes.mit.edu/burgelab/miso/ as human genome (hg19) alternative events v1.0). Standard analysis parameters were used, with a filter option applied to require a minimum of 20 reads to support an event identification.

To identify regulatory elements that may affect retention of EIF2B5 intron 12 we used AVISPA (105). This method, based on computationally derived splicing codes, has been

used previously to detect and experimentally verify novel regulators of exon splicing in a variety of experimental conditions (122-124). Since AVISPA was built for analyzing differential splicing determinants around cassette exons we extracted hg19 coordinates for Ensembl-defined exons 11-13 and 12-14, then analyzed these two triplet exons genomic regions via AVISPA. Also tested were exon triplets 6-8, 7-9, 8-10, and 9-11 to serve as negative controls as these exons are known to be constitutive and not exhibit intron retention. The splicing related top motifs and regulatory features were defined by their normalized feature effect (NFE) and their relative enrichment compared to alternative and constitutive exons. Briefly, the NFE value represents the effect on splicing prediction outcome if a motif is removed in silico, normalized by the total effects observed from removing each of the top features in this way.

RT-PCR

PCR reactions were carried out with cDNA prepared from RNA treated with DNAseI (Qiagen) to minimize contamination of DNA and in a reverse transcription reaction using oligo-dT primers to enrich for mature mRNA. Reverse transcription was carried out according to manufacturer's protocol (Taqman RT reagents). PCR reactions were carried out in a PTC-100 Thermocycler (MJ Research, Inc.) for 40 cycles, using annealing temperatures optimal for each primer set. Quantitative PCR reactions were prepared using Power SYBR Green PCR Master Mix (Applied Biosystems) and carried out on a QuantStudio 6 Flex Real-Time PCR Instrument (Thermo Fisher Scientific).

RNAi and expression plasmid experiments

SQ20B cells were plated 24-48h before transfection and grown to approximately 60-70% confluency. RNAi transfections were carried out using a mixure of lipofectamine RNAi

Max (ThermoFisher) diluted in OptiMEM media with siRNA to 10-50nM, which was added to cell culture plates in complete DMEM. Cells were placed in incubator for 24h, at which point the media was replaced. After an additional 24h, cells either harvested or used for subsequent experiments. For expression experiments, plasmids were purchased from Origene. Site-directed mutagenesis was used to alter the original plasmid and introduce a TAG stop codon, and confirmed by Sanger sequencing (see Figure 6A). Expression plasmids were transfected in cells plated to the same confluency as described above using a mixture of lipofectamine 2000 reagent (ThermoFisher) diluted in OptiMEM media with varying concentrations of pCMV expression plasmid added to cells in complete DMEM. The plates of cells were incubated for 4-12h, at which point the media was washed off and replaced. Cells were harvested or used for downstream experiments 24-48h post-transfection.

Immunoblot analyses

Whole cell lysates were collected using a lysis buffer of 2% Triton-X, 1X Complete Mini protease inhibitor cocktail (Roche) and 1X phosphatase inhibitor cocktail 2 (Sigma) in PBS. The nuclear/cytosol fractionation reagents (BioVision) supplemented with 1X phosphatase inhibitor cocktail 2(Sigma) were used to extract cytoplasmic and nuclear extracts from the same sample. Lysates isolated from frozen tumor and normal mouse tissue were lysed in a buffer containing: 1% Triton X-100, 50mM HEPES, ph 7.4, 150mM NaCl, 1.5mM MgCl2, 1mM EGTA, 100mM NaF, 10mM Na pyrophosphate, 1mM Na3VO4, 10% glycerol, protease inhibitors (Roche #04693116001) and phosphatase inhibitors (Roche #04906845001). All protein concentrations were determined using DC protein assay (BioRad). Equal amounts of protein were resolved on 10% or 12% sodium dodecyl sulfate polyacrylamide gels and transferred to polyvinylidene fluoride

membranes. Membranes were blocked with 5% non-fat dried milk in TBS-T (20 mM Tris, 137 mM NaCl, 0.1% Tween-20; pH 7.6) and then incubated in a 1:1000 dilution of primary antibody in 5% milk/TBS-T followed by 1:5000 dilution of secondary antibody in 5% milk/TBS-T. After washing, membranes were treated with ECL chemicals and exposed to autoradiograph film.

Liquid chromatography tandem mass-spectrometry

The LC-MS/MS was carried out at the Wistar core facility. Complete protocol available online: https://www.wistar.org/our-science/shared-facilities/proteomics-facility/helpful-information.

^{35}S labeling for measurement of protein synthesis/image quantification

Following transfection experiment, SQ20B cells were incubated with methionine/cysteine-free media for 30m. For labeling, one set of experimental cell plates were incubated for 30m with media supplemented with 0.075 mCi/ml [35S]-methionine/cysteine, while a second set of plates were incubated with “cold” media supplemented with non-radioactive 1X methionine/cysteine. Protein was harvested from the “cold” samples and a protein assay was performed to obtain concentrations. These proteins were analyzed using standard immunoblot assay conditions. Proteins collected from the [35S]-methionine/cysteine labeled cells were resolved on SDS-PAGE. The resulting gel was then fixed using a solution of 20% methanol and 10% acetic acid for 30m, washed with deionized water, and then incubated on a rocker at room-temperature with enlightening solution (PerkinElmer) for 15-30m. The gel was then dried for 16h using a Bio-Rad gel drying apparatus and then exposed to autoradiography film at -80°C for 2h before processing.

Polysome profiling

Polysome profiling was carried out per previously described conditions (125).

Chromatin immunoprecipitation

For ChIP experiments, SQ20B cells were plated 24h before placing into hypoxia chamber or standard incubator. Six 10cm plates at 70% confluency were grown in normoxic or hypoxic (0.5% O_2) conditions for 16h, at which time cells were crosslinked for 10m at room temperature using 1% formaldehyde in minimum essential medium. Crosslinking was stopped and cells were washed and lysed according to manufacturer's protocol (Active Motif ChIP kit #53035). Shearing conditions were carried out for six 20s pulses at 25% power, with 30s rest in between pulses on ice. Immunoprecipitations were carried out according to protocol, with 40ug chromatin and 3ug antibody for RNAPII (Active Motif #39097, mouse IgG #53010) and 60ug chromatin with 3ug (rabbit IgG Santa Cruz #sc-2027X) or 30ug P-Ser2 RNAPII (Abcam #5095). For the resulting qPCR reactions, primers specific to *EIF2B5* intron 10 and intron 12 were used (Table S1), and control primers were purchased from Active Motif (GAPDH-2 for RNAPII control #71006, GAPDH-1 for P-Ser2 RNAPII control #71004, and Negative-1 for a 78bp intergenic region of chromosome 12 as a negative control #71001).

RNA immunoprecipitation

SQ20B cells were grown in 2 x 150cm tissue culture plates for each condition (normoxia and a 0.5% hypoxia time-point). Antibody against SRSF3 (SRp20) was purchased from MBL, Inc. (#RN080PW). Rabbit IgG was provided by the RIP kit for use as a control (RIP Assay kit, MBL, Inc. # RN1001). Protein A Sepharose CL-4B (GE Healthcare) were prepared fresh for the beginning of the experiment in a slurry of 75% beads in 25%

50mM Tris pH 7.5. Beads were pre-washed in PBS before adding 15µg of antibody and then incubated at 4 degrees with rotation for 4h. At this time, beads were pre-washed before lysing cells and adding the lysates to the Protein A beads to preclear for 1h at 4 degrees with rotation. Input samples were collected at this time before adding the precleared lysate to the antibody-bound beads. Samples were incubated for 3h at 4 degrees with rotation. After wash steps, samples were aliquoted for quality control analysis of the protein. RNA was isolated according to the manufacturer's protocol and analyzed using the Nanodrop1000 UV spectrometer. Equal amounts of RNA were then processed into cDNA and used for subsequent qPCR analysis. Input RNA was used as a standard to calculate the quantity for each primer. Expression data are reported as the relative enrichment of SRSF3 immunoprecipitation over the control Rabbit IgG immunoprecipitation.

Data Availability

All RNA-sequencing files and analyzed gene expression results have been deposited into the Gene Expression Omnibus as GSE87456. Any other data used in the preparation of this study can be issued upon request from Dr. Koumenis.

Acknowledgements

We would like to acknowledge the Vivian Cheung lab at the University of Michigan for their assistance with the RNA-sequencing, Dr. Vladimir Popov and the Amit Maity lab for technical assistance, Dr. John Tobias at the Molecular Profiling Core at The University of Pennsylvania for support with data analysis, and Drs. Hsin-Yao Tang and David Speicher of the Wistar Proteomics facility for assistance with the mass-spectrometry experiments and analysis. This project was partially supported by a pilot grant from The

Abramson Cancer Center, University of Pennsylvania and also supported by an NIH grant-CA094214. The authors acknowledge there are no conflicts of interest to report.

BIBLIOGRAPHY

1. Yeo GW, Van Nostrand EL, Liang TY. Discovery and analysis of evolutionarily conserved intronic splicing regulatory elements. PLoS Genetics. 2007;3(5):814-29.
2. Meininghaus M, Chapman RD, Horndasch M, Eick D. Conditional expression of RNA polymerase II in mammalian cells. Deletion of the carboxyl-terminal domain of the large subunit affects early steps in transcription2000. 24375-82 p.
3. Wong JJL, Ritchie W, Ebner Oa, Selbach M, Wong JWH, Huang Y, et al. Orchestrated intron retention regulates normal granulocyte differentiation. Cell. 2013;154(3):583-95.
4. Vaupel P, Kallinowski F, Okunieff P. Blood flow, oxygen and nutrient supply, and metabolic microenvironment of human tumors: a review. Cancer Res. 1989;49(23):6449-65.
5. Hockel M, Schlenger K, Aral B, Mitze M, Schaffer U, Vaupel P. Association between tumor hypoxia and malignant progression in advanced cancer of the uterine cervix. Cancer Res. 1996;56(19):4509-15.
6. Hu YL, Jahangiri A, De Lay M, Aghi MK. Hypoxia-induced tumor cell autophagy mediates resistance to anti-angiogenic therapy. Autophagy. 2012;8(6):979-81.
7. Bhattacharya A, Toth K, Mazurchuk R, Spernyak JA, Slocum HK, Pendyala L, et al. Lack of microvessels in well-differentiated regions of human head and neck squamous cell carcinoma A253 associated with functional magnetic resonance imaging detectable hypoxia, limited drug delivery, and resistance to irinotecan therapy. Clinical cancer research : an official journal of the American Association for Cancer Research. 2004;10(23):8005-17.
8. Koumenis C, Naczki C, Rastani S, Diehl A, Sonenberg N, Koromilas A, et al. Regulation of Protein Synthesis by Hypoxia via Activation of the Endoplasmic Reticulum Kinase PERK and Phosphorylation of the Translation Initiation Factor eIF2 α Regulation of Protein Synthesis by Hypoxia via Activation of the Endoplasmic Reticulum Kinas. Molecular and cellular biology. 2002;22(21):7405-16.
9. Koumenis C, Maxwell PH. Low oxygen stimulates the intellect. Symposium on hypoxia and development, physiology and disease. EMBO reports. 2006;7(7):679-84.
10. Vaupel P, Mayer A. Hypoxia in cancer: significance and impact on clinical outcome. Cancer metastasis reviews. 2007;26(2):225-39.
11. Rofstad EK, Gaustad JV, Egeland TA, Mathiesen B, Galappathi K. Tumors exposed to acute cyclic hypoxic stress show enhanced angiogenesis, perfusion and metastatic dissemination. International journal of cancer Journal international du cancer. 2010;127(7):1535-46.
12. Maftei CA, Bayer C, Shi K, Astner ST, Vaupel P. Quantitative assessment of hypoxia subtypes in microcirculatory supply units of malignant tumors using (immuno-)fluorescence techniques. Strahlentherapie und Onkologie : Organ der Deutschen Rontgengesellschaft [et al]. 2011;187(4):260-6.
13. Vaupel P, Mayer A. Hypoxia in tumors: pathogenesis-related classification, characterization of hypoxia subtypes, and associated biological and clinical implications. Advances in experimental medicine and biology. 2014;812:19-24.

14. Vaupel P, Mayer A, Höckel M. Tumor Hypoxia and Malignant Progression. In: Chandan KS, Gregg LS, editors. Methods in enzymology. Volume 381: Academic Press; 2004. p. 335-54.
15. Laderoute KR, Alarcon RM, Brody MD, Calaoagan JM, Chen EY, Knapp AM, et al. Opposing effects of hypoxia on expression of the angiogenic inhibitor thrombospondin 1 and the angiogenic inducer vascular endothelial growth factor. Clinical cancer research : an official journal of the American Association for Cancer Research. 2000;6(7):2941-50.
16. Rampling R, Cruickshank G, Lewis AD, Fitzsimmons SA, Workman P. Direct measurement of pO2 distribution and bioreductive enzymes in human malignant brain tumors. International journal of radiation oncology, biology, physics. 1994;29(3):427-31.
17. Brizel DM, Scully SP, Harrelson JM, Layfield LJ, Bean JM, Prosnitz LR, et al. Tumor oxygenation predicts for the likelihood of distant metastases in human soft tissue sarcoma. Cancer Res. 1996;56(5):941-3.
18. Nordsmark M, Overgaard M, Overgaard J. Pretreatment oxygenation predicts radiation response in advanced squamous cell carcinoma of the head and neck. Radiotherapy and oncology : journal of the European Society for Therapeutic Radiology and Oncology. 1996;41(1):31-9.
19. Komar G, Lehtiö K, Seppänen M, Eskola O, Levola H, Lindholm P, et al. Prognostic value of tumour blood flow, [18F]EF5 and [18F]FDG PET/CT imaging in patients with head and neck cancer treated with radiochemotherapy. European Journal of Nuclear Medicine and Molecular Imaging. 2014.
20. Buffa FM, Harris AL, West CM, Miller CJ. Large meta-analysis of multiple cancers reveals a common, compact and highly prognostic hypoxia metagene. Br J Cancer. 2010;102(2):428-35.
21. Winter SC, Buffa FM, Silva P, Miller C, Valentine HR, Turley H, et al. Relation of a hypoxia metagene derived from head and neck cancer to prognosis of multiple cancers. Cancer Res. 2007;67(7):3441-9.
22. Denko NC, Fontana LA, Hudson KM, Sutphin PD, Raychaudhuri S, Altman R, et al. Investigating hypoxic tumor physiology through gene expression patterns. Oncogene. 2003;22(37):5907-14.
23. Denko N, Wernke-Dollries K, Johnson AB, Hammond E, Chiang CM, Barton MC. Hypoxia actively represses transcription by inducing negative cofactor 2 (Dr1/DrAP1) and blocking preinitiation complex assembly. Journal of Biological Chemistry. 2003;278(8):5744-9.
24. Tang X, Lucas JE, Chen JL, LaMonte G, Wu J, Wang MC, et al. Functional interaction between responses to lactic acidosis and hypoxia regulates genomic transcriptional outputs. Cancer Res. 2012;72(2):491-502.
25. Marotta D, Karar J, Jenkins WT, Kumanova M, Jenkins KW, Tobias JW, et al. In vivo profiling of hypoxic gene expression in gliomas using the hypoxia marker EF5 and laser-capture microdissection. Cancer Research. 2011;71(3):779-89.
26. Koch CJ, Hahn SM, Rockwell K, Jr., Covey JM, McKenna WG, Evans SM. Pharmacokinetics of EF5 [2-(2-nitro-1-H-imidazol-1-yl)-N-(2,2,3,3,3-pentafluoropropyl) acetamide] in human patients: implications for hypoxia measurements in vivo by 2-nitroimidazoles. Cancer chemotherapy and pharmacology. 2001;48(3):177-87.
27. Alberts B, Johnson A, Lewis J, al. e. Molecular Biology of the Cell. 4th edition. New York: Garland Science; 2002.

28. Semenza GL. Hydroxylation of HIF-1: oxygen sensing at the molecular level. Physiology (Bethesda, Md). 2004;19:176-82.
29. Tatum JL, Kelloff GJ, Gillies RJ, Arbeit JM, Brown JM, Chao KS, et al. Hypoxia: importance in tumor biology, noninvasive measurement by imaging, and value of its measurement in the management of cancer therapy. International journal of radiation biology. 2006;82(10):699-757.
30. Weinmann M, Belka C, Guner D, Goecke B, Muller I, Bamberg M, et al. Array-based comparative gene expression analysis of tumor cells with increased apoptosis resistance after hypoxic selection. Oncogene. 2005;24(38):5914-22.
31. Pawlus MR, Wang L, Hu CJ. STAT3 and HIF1[alpha] cooperatively activate HIF1 target genes in MDA-MB-231 and RCC4 cells. Oncogene. 2014;33(13):1670-9.
32. Bristow RG, Hill RP. Hypoxia and metabolism. Hypoxia, DNA repair and genetic instability. Nat Rev Cancer. 2008;8(3):180-92.
33. Kulshreshtha R, Ferracin M, Wojcik SE, Garzon R, Alder H, Agosto-Perez FJ, et al. A microRNA signature of hypoxia. Mol Cell Biol. 2007;27(5):1859-67.
34. Gardner LB, Corn PG. Hypoxic regulation of mRNA expression. Cell cycle (Georgetown, Tex). 2008;7(13):1916-24.
35. Voellenkle C, Rooij J, Guffanti A, Brini E, Fasanaro P, Isaia E, et al. Deep-sequencing of endothelial cells exposed to hypoxia reveals the complexity of known and novel microRNAs. RNA (New York, NY). 2012;18(3):472-84.
36. Galban S, Kuwano Y, Pullmann R, Jr., Martindale JL, Kim HH, Lal A, et al. RNA-binding proteins HuR and PTB promote the translation of hypoxia-inducible factor 1alpha. Mol Cell Biol. 2008;28(1):93-107.
37. Schepens B, Tinton SA, Bruynooghe Y, Beyaert R, Cornelis S. The polypyrimidine tract-binding protein stimulates HIF-1alpha IRES-mediated translation during hypoxia. Nucleic Acids Res. 2005;33(21):6884-94.
38. Zhang LF, Lou JT, Lu MH, Gao C, Zhao S, Li B, et al. Suppression of miR-199a maturation by HuR is crucial for hypoxia-induced glycolytic switch in hepatocellular carcinoma. Embo j. 2015;34(21):2671-85.
39. Gardner LB. Hypoxic inhibition of nonsense-mediated RNA decay regulates gene expression and the integrated stress response. Mol Cell Biol. 2008;28(11):3729-41.
40. Harding HP, Novoa I, Zhang Y, Zeng H, Wek R, Schapira M, et al. Regulated translation initiation controls stress-induced gene expression in mammalian cells. Mol Cell. 2000;6(5):1099-108.
41. Zhan K, Narasimhan J, Wek RC. Differential activation of eIF2 kinases in response to cellular stresses in Schizosaccharomyces pombe. Genetics. 2004;168(4):1867-75.
42. Popp MW, Maquat LE. Organizing principles of mammalian nonsense-mediated mRNA decay. Annual review of genetics. 2013;47:139-65.
43. Baek D, Green P. Sequence conservation, relative isoform frequencies, and nonsense-mediated decay in evolutionarily conserved alternative splicing. Proc Natl Acad Sci U S A. 2005;102(36):12813-8.
44. Green RE, Lewis BP, Hillman RT, Blanchette M, Lareau LF, Garnett AT, et al. Widespread predicted nonsense-mediated mRNA decay of alternatively-spliced transcripts of human normal and disease genes. Bioinformatics. 2003;19 Suppl 1:i118-21.
45. Gardner LB. Nonsense-mediated RNA decay regulation by cellular stress: implications for tumorigenesis. Mol Cancer Res. 2010;8(3):295-308.

46. Singh LP, Aroor AR, Wahba AJ. Translational control of eukaryotic gene expression. Role of the guanine nucleotide exchange factor and chain initiation factor-2. Enzyme & protein. 1994;48(2):61-80.
47. Gomez E, Pavitt GD. Identification of domains and residues within the epsilon subunit of eukaryotic translation initiation factor 2B (eIF2Bepsilon) required for guanine nucleotide exchange reveals a novel activation function promoted by eIF2B complex formation. Mol Cell Biol. 2000;20(11):3965-76.
48. Novoa I, Zeng H, Harding HP, Ron D. Feedback inhibition of the unfolded protein response by GADD34-mediated dephosphorylation of eIF2alpha. The Journal of cell biology. 2001;153(5):1011-22.
49. Koritzinsky M, Magagnin MG, van den Beucken T, Seigneuric R, Savelkouls K, Dostie J, et al. Gene expression during acute and prolonged hypoxia is regulated by distinct mechanisms of translational control. Embo j. 2006;25(5):1114-25.
50. Sena Ja, Wang L, Heasley LE, Hu C-J. Hypoxia Regulates Alternative Splicing of HIF and non-HIF Target Genes. Molecular cancer research : MCR. 2014:1233-43.
51. Memon D, Dawson K, Smowton C, Xing W, Dive C, Miller C. Hypoxia-driven splicing into noncoding isoforms regulates the DNA damage response. npj Genomic Medicine. 2016.
52. Sena Ja, Wang L, Pawlus MR, Hu C-J. HIFs enhance the transcriptional activation and splicing of adrenomedullin. Molecular cancer research : MCR. 2014;12(5):728-41.
53. Oltean S, Bates DO. Hallmarks of alternative splicing in cancer. Oncogene. 2013(November):1-8.
54. Jakubauskiene E, Vilys L, Makino Y, Poellinger L, Kanopka A. Increased Serine-Arginine (SR) Protein Phosphorylation Changes Pre-mRNA Splicing in Hypoxia. J Biol Chem. 2015;290(29):18079-89.
55. Mirtschink P, Krishnan J, Grimm F, Sarre A, Horl M, Kayikci M, et al. HIF-driven SF3B1 induces KHK-C to enforce fructolysis and heart disease. Nature. 2015;522(7557):444-9.
56. Jurica MS, Moore MJ. Pre-mRNA splicing: awash in a sea of proteins. Mol Cell. 2003;12(1):5-14.
57. Wahl MC, Will CL, Luhrmann R. The spliceosome: design principles of a dynamic RNP machine. Cell. 2009;136(4):701-18.
58. Graveley BR, Hertel KJ, Maniatis T. A systematic analysis of the factors that determine the strength of pre-mRNA splicing enhancers. Embo j. 1998;17(22):6747-56.
59. Graveley BR, Maniatis T. Arginine/serine-rich domains of SR proteins can function as activators of pre-mRNA splicing. Molecular cell. 1998;1(5):765-71.
60. Krecic AM, Swanson MS. hnRNP complexes: composition, structure, and function. Curr Opin Cell Biol. 1999;11(3):363-71.
61. Fong N, Kim H, Zhou Y, Ji X, Qiu J, Saldi T, et al. Pre-mRNA splicing is facilitated by an optimal RNA polymerase II elongation rate. Genes Dev. 2014;28(23):2663-76.
62. Dvinge H, Kim E, Abdel-Wahab O, Bradley RK. RNA splicing factors as oncoproteins and tumour suppressors. Nat Rev Cancer. 2016;16(7):413-30.
63. Matera AG, Wang Z. A day in the life of the spliceosome. Nat Rev Mol Cell Biol. 2014;15(2):108-21.

64. Anczukow O, Rosenberg AZ, Akerman M, Das S, Zhan L, Karni R, et al. The splicing factor SRSF1 regulates apoptosis and proliferation to promote mammary epithelial cell transformation. Nat Struct Mol Biol. 2012;19(2):220-8.
65. Tang Y, Horikawa I, Ajiro M, Robles AI, Fujita K, Mondal AM, et al. Downregulation of splicing factor SRSF3 induces p53beta, an alternatively spliced isoform of p53 that promotes cellular senescence. Oncogene. 2013;32(22):2792-8.
66. Dvinge H, Bradley RK. Widespread intron retention diversifies most cancer transcriptomes. Genome medicine. 2015;7(1):45.
67. Danan-Gotthold M, Golan-Gerstl R, Eisenberg E, Meir K, Karni R, Levanon EY. Identification of recurrent regulated alternative splicing events across human solid tumors. Nucleic Acids Res. 2015;43(10):5130-44.
68. Komar G, Seppänen M, Eskola O, Lindholm P, Grönroos TJ, Forsback S, et al. 18F-EF5: a new PET tracer for imaging hypoxia in head and neck cancer. Journal of nuclear medicine : official publication, Society of Nuclear Medicine. 2008;49(12):1944-51.
69. Wang ET, Sandberg R, Luo S, Khrebtukova I, Zhang L, Mayr C, et al. Alternative isoform regulation in human tissue transcriptomes. Nature. 2008;456(7221):470-6.
70. Pan Q, Shai O, Lee LJ, Frey BJ, Blencowe BJ. Deep surveying of alternative splicing complexity in the human transcriptome by high-throughput sequencing. Nat Genet. 2008;40(12):1413-5.
71. Koch CJ. Measurement of absolute oxygen levels in cells and tissues using oxygen sensors and 2-nitroimidazole EF5. Methods in enzymology. 2002;352:3-31.
72. Dobin A, Davis CA, Schlesinger F, Drenkow J, Zaleski C, Jha S, et al. STAR: ultrafast universal RNA-seq aligner. Bioinformatics. 2013;29(1):15-21.
73. Trapnell C, Williams BA, Pertea G, Mortazavi A, Kwan G, van Baren MJ, et al. Transcript assembly and quantification by RNA-Seq reveals unannotated transcripts and isoform switching during cell differentiation. Nature biotechnology. 2010;28(5):511-5.
74. Erichsen DA, Armstrong MB, Wechsler DS. Mxi1 and mxi1-0 antagonize N-myc function and independently mediate apoptosis in neuroblastoma. Translational oncology. 2015;8(1):65-74.
75. Armstrong MB, Mody RJ, Ellis DC, Hill AB, Erichsen DA, Wechsler DS. N-Myc differentially regulates expression of MXI1 isoforms in neuroblastoma. Neoplasia (New York, NY). 2013;15(12):1363-70.
76. Khurana P, Sugadev R, Jain J, Singh SB. HypoxiaDB: a database of hypoxia-regulated proteins. Database : the journal of biological databases and curation. 2013;2013:bat074.
77. Wang Y, Kuramitsu Y, Kitagawa T, Baron B, Yoshino S, Maehara S, et al. Cofilin-phosphatase slingshot-1L (SSH1L) is over-expressed in pancreatic cancer (PC) and contributes to tumor cell migration. Cancer letters. 2015;360(2):171-6.
78. Chakraborty A, Werner JK, Jr., Koldobskiy MA, Mustafa AK, Juluri KR, Pietropaoli J, et al. Casein kinase-2 mediates cell survival through phosphorylation and degradation of inositol hexakisphosphate kinase-2. Proc Natl Acad Sci U S A. 2011;108(6):2205-9.
79. Schodel J, Oikonomopoulos S, Ragoussis J, Pugh CW, Ratcliffe PJ, Mole DR. High-resolution genome-wide mapping of HIF-binding sites by ChIP-seq. Blood. 2011;117(23):e207-17.
80. Blencowe BJ. Alternative splicing: new insights from global analyses. Cell. 2006;126(1):37-47.

81. Huang D, Sherman BT, Lempicki RA. Systematic and integrative analysis of large gene lists using DAVID bioinformatics resources. Nat Protoc. 2009;4(1):44-57.
82. Ghalayini MK, Dong Q, Richardson DR, Assinder SJ. Proteolytic cleavage and truncation of NDRG1 in human prostate cancer cells, but not normal prostate epithelial cells. Bioscience reports. 2013;33(3).
83. Donato MD, Fanelli M, Mariani M, Raspaglio G, Pandya D, He S, et al. Nek6 and Hif-1alpha cooperate with the cytoskeletal gateway of drug resistance to drive outcome in serous ovarian cancer. American journal of cancer research. 2015;5(6):1862-77.
84. Lofstedt T, Fredlund E, Noguera R, Navarro S, Holmquist-Mengelbier L, Beckman S, et al. HIF-1alpha induces MXI1 by alternate promoter usage in human neuroblastoma cells. Experimental cell research. 2009;315(11):1924-36.
85. Katz Y, Wang ET, Airoldi EM, Burge CB. Analysis and design of RNA sequencing experiments for identifying isoform regulation. Nat Methods. 2010;7(12):1009-15.
86. Semenza GL. Molecular mechanisms mediating metastasis of hypoxic breast cancer cells. Trends in molecular medicine. 2012;18(9):534-43.
87. Harris AL. Hypoxia--a key regulatory factor in tumour growth. Nat Rev Cancer. 2002;2(1):38-47.
88. Evans SM, Joiner B, Jenkins WT, Laughlin KM, Lord EM, Koch CJ. Identification of hypoxia in cells and tissues of epigastric 9L rat glioma using EF5 [2-(2-nitro-1H-imidazol-1-yl)-N-(2,2,3,3,3-pentafluoropropyl) acetamide]. British journal of cancer. 1995;72(4):875-82.
89. Erapaneedi R, Belousov VV, Schafers M, Kiefer F. A novel family of fluorescent hypoxia sensors reveal strong heterogeneity in tumor hypoxia at the cellular level. Embo j. 2016;35(1):102-13.
90. Brady LK, Popov V, Koumenis C. In Vivo Interrogation of the Hypoxic Transcriptome of Solid Tumors: Optimizing Hypoxic Probe Labeling with Laser Capture Microdissection for Isolation of High-Quality RNA for Deep Sequencing Analysis. Advances in experimental medicine and biology. 2016;899:41-58.
91. LaGory EL, Giaccia AJ. The ever-expanding role of HIF in tumour and stromal biology. Nat Cell Biol. 2016;18(4):356-65.
92. Galbraith MD, Allen Ma, Bensard CL, Wang X, Schwinn MK, Qin B, et al. XHIF1A employs CDK8-mediator to stimulate RNAPII elongation in response to hypoxia. Cell. 2013;153(6):1327-39.
93. Choudhry H, Schodel J, Oikonomopoulos S, Camps C, Grampp S, Harris A, et al. Extensive regulation of the non-coding transcriptome by hypoxia: role of HIF in releasing RNApol2. EMBO reports. 2013;15(1):70-6.
94. de la Mata M, Alonso CR, Kadener S, Fededa JP, Blaustein M, Pelisch F, et al. A slow RNA polymerase II affects alternative splicing in vivo. Mol Cell. 2003;12(2):525-32.
95. Jimeno-Gonzalez S, Payan-Bravo L, Munoz-Cabello AM, Guijo M, Gutierrez G, Prado F, et al. Defective histone supply causes changes in RNA polymerase II elongation rate and cotranscriptional pre-mRNA splicing. Proc Natl Acad Sci U S A. 2015;112(48):14840-5.
96. Hicks MJ, Yang CR, Kotlajich MV, Hertel KJ. Linking splicing to Pol II transcription stabilizes pre-mRNAs and influences splicing patterns. PLoS Biol. 2006;4(6):e147.
97. Bi M, Naczki C, Koritzinsky M, Fels D, Blais J, Hu N, et al. ER stress-regulated translation increases tolerance to extreme hypoxia and promotes tumor growth. Embo j. 2005;24(19):3470-81.

98. Ortiz-Barahona A, Villar D, Pescador N, Amigo J, del Peso L. Genome-wide identification of hypoxia-inducible factor binding sites and target genes by a probabilistic model integrating transcription-profiling data and in silico binding site prediction. Nucleic Acids Res. 2010;38(7):2332-45.
99. Hanzelmann P, Schindelin H. The structural and functional basis of the p97/valosin-containing protein (VCP)-interacting motif (VIM): mutually exclusive binding of cofactors to the N-terminal domain of p97. J Biol Chem. 2011;286(44):38679-90.
100. Heo JM, Livnat-Levanon N, Taylor EB, Jones KT, Dephoure N, Ring J, et al. A stress-responsive system for mitochondrial protein degradation. Mol Cell. 2010;40(3):465-80.
101. Vaquero-Garcia J, Barrera A, Gazzara MR, Gonzalez-Vallinas J, Lahens NF, Hogenesch JB, et al. A new view of transcriptome complexity and regulation through the lens of local splicing variations. eLife. 2016;5:e11752.
102. Brizel DM, Sibley GS, Prosnitz LR, Scher RL, Dewhirst MW. Tumor hypoxia adversely affects the prognosis of carcinoma of the head and neck. International journal of radiation oncology, biology, physics. 1997;38(2):285-9.
103. Nordsmark M, Bentzen SM, Rudat V, Brizel D, Lartigau E, Stadler P, et al. Prognostic value of tumor oxygenation in 397 head and neck tumors after primary radiation therapy. An international multi-center study. Radiotherapy and oncology : journal of the European Society for Therapeutic Radiology and Oncology. 2005;77(1):18-24.
104. Saltzman AL, Pan Q, Blencowe BJ. Regulation of alternative splicing by the core spliceosomal machinery. Genes & Development. 2011;25(4):373-84.
105. Barash Y, Vaquero-Garcia J, González-Vallinas J, Xiong HY, Gao W, Lee LJ, et al. AVISPA: a web tool for the prediction and analysis of alternative splicing. Genome Biology. 2013;14(10):R114-R.
106. Barash Y, Calarco JA, Gao W, Pan Q, Wang X, Shai O, et al. Deciphering the splicing code. Nature. 2010;465(7294):53-9.
107. Gooding C, Clark F, Wollerton MC, Grellscheid SN, Groom H, Smith CW. A class of human exons with predicted distant branch points revealed by analysis of AG dinucleotide exclusion zones. Genome Biol. 2006;7(1):R1.
108. de la Mata MD, Alonso CR, Fededa JP, Pelisch F, Cramer P, Bentley D, et al. Affects Alternative Splicing In Vivo. 2003;12:525-32.
109. Luco RF, Allo M, Schor IE, Kornblihtt AR, Misteli T. Epigenetics in alternative pre-mRNA splicing. Cell. 2011;144(1):16-26.
110. Braunschweig U, Barbosa-Morais NL, Pan Q, Nachman EN, Alipanahi B, Gonatopoulos-Pournatzis T, et al. Widespread intron retention in mammals functionally tunes transcriptomes. Genome Research. 2014;24(11):1774-86.
111. Gomez E, Pavitt G. of Eukaryotic Translation Initiation Factor 2B (eIF2Bε) Required for Guanine Nucleotide Exchange Reveals a Novel Activation Function Promoted by eIF2B Complex. Molecular and cellular biology. 2000.
112. Jennings MD, Kershaw CJ, Adomavicius T, Pavitt GD. Fail-safe control of translation initiation by dissociation of eIF2alpha phosphorylated ternary complexes. eLife. 2017;6.
113. Sakabe NJ, de Souza SJ. Sequence features responsible for intron retention in human. BMC genomics. 2007;8:59.

114. Amit M, Donyo M, Hollander D, Goren A, Kim E, Gelfman S, et al. Differential GC content between exons and introns establishes distinct strategies of splice-site recognition. Cell Rep. 2012;1(5):543-56.
115. Gu B, Eick D, Bensaude O. CTD serine-2 plays a critical role in splicing and termination factor recruitment to RNA polymerase II in vivo. Nucleic Acids Research. 2013;41(3):1591-603.
116. Egloff S, Dienstbier M, Murphy S. Updating the RNA polymerase CTD code: adding gene-specific layers. Trends in genetics : TIG. 2012;28(7):333-41.
117. Pineda G, Shen Z, de Albuquerque CP, Reynoso E, Chen J, Tu CC, et al. Proteomics studies of the interactome of RNA polymerase II C-terminal repeated domain. BMC research notes. 2015;8:616.
118. Munoz MJ, Perez Santangelo MS, Paronetto MP, de la Mata M, Pelisch F, Boireau S, et al. DNA damage regulates alternative splicing through inhibition of RNA polymerase II elongation. Cell. 2009;137(4):708-20.
119. Ye J, Kumanova M, Hart LS, Sloane K, Zhang H, De Panis DN, et al. The GCN2-ATF4 pathway is critical for tumour cell survival and proliferation in response to nutrient deprivation. Embo j. 2010;29(12):2082-96.
120. Leegwater PA, Vermeulen G, Konst AA, Naidu S, Mulders J, Visser A, et al. Subunits of the translation initiation factor eIF2B are mutant in leukoencephalopathy with vanishing white matter. Nat Genet. 2001;29(4):383-8.
121. Balachandran S, Barber GN. Defective translational control facilitates vesicular stomatitis virus oncolysis. Cancer Cell. 2004;5(1):51-65.
122. Sotillo E, Barrett DM, Black KL, Bagashev A, Oldridge D, Wu G, et al. Convergence of Acquired Mutations and Alternative Splicing of CD19 Enables Resistance to CART-19 Immunotherapy. Cancer discovery. 2015;5(12):1282-95.
123. Melamed Z, Levy A, Ashwal-Fluss R, Lev-Maor G, Mekahel K, Atias N, et al. Alternative splicing regulates biogenesis of miRNAs located across exon-intron junctions. Mol Cell. 2013;50(6):869-81.
124. Xiong HY, Alipanahi B, Lee LJ, Bretschneider H, Merico D, Yuen RK, et al. RNA splicing. The human splicing code reveals new insights into the genetic determinants of disease. Science. 2015;347(6218):1254806.
125. Johannes G, Sarnow P. Cap-independent polysomal association of natural mRNAs encoding c-myc, BiP, and eIF4G conferred by internal ribosome entry sites. RNA (New York, NY). 1998;4(12):1500-13.